

1 **A Critical Review on the Vulnerability Assessment of Natural Gas**
2 **Pipelines Subjected to Seismic Wave Propagation. Part 1: Fragility**
3 **Relations and Implemented Seismic Intensity Measures**

4
5 **Grigorios Tsinidis¹, Luigi Di Sarno², Anastasios Sextos³, and Peter Furtner⁴**

6
7 ¹University of Sannio, Italy & Vienna Consulting Engineers ZT GmbH, Austria

8 ²University of Liverpool, United Kingdom & University of Sannio, Italy

9 ³University of Bristol, United Kingdom & Aristotle University of Thessaloniki, Greece

10 ⁴Vienna Consulting Engineers ZT GmbH, Austria

11
12 **Corresponding Author:** Grigorios Tsinidis, University of Sannio, School of Engineering,
13 Piazza Roma, 21, 82100, Benevento, Italy, email: tsinidis.grigorios@gmail.com

14
15 **Abstract:** Natural gas (NG) pipeline networks constitute a critical means of energy
16 transportation, playing a vital role in the economic development of modern societies. The
17 associated socioeconomic and environmental impact, in case of seismically-induced severe
18 damages, highlights the importance of a rational assessment of the structural integrity of this
19 infrastructure against seismic hazards. Up to date, this assessment is mainly performed by
20 implementing empirical fragility relations, which associate the repair rate, i.e. the number of
21 repairs/damages per unit length of the pipeline, with a seismic intensity measure. A limited
22 number of analytical fragility curves that compute probabilities of failure for various levels of
23 predefined damage states have also been proposed, recently. In the first part of this paper, a
24 thorough critical review of available fragility relations for the vulnerability assessment of
25 buried NG pipelines is presented. The paper focuses on the assessment against seismically-
26 induced transient ground deformations, which, under certain circumstances, may induce non-
27 negligible deformations and strains on buried NG pipelines, especially in cases of pipelines
28 crossing heterogeneous soil sites. Particular emphasis is placed on the efficiency of
29 implemented seismic intensity measures to be evaluated or measured in the field and, more
30 importantly, to correlate with observed structural damages on buried NG pipelines. In the
31 second part of this paper, alternative methods for the analytical evaluation of the fragility of
32 steel NG pipelines under seismically-induced transient ground deformations are presented.
33 Through the discussion, recent advancements in the field are highlighted, whilst acknowledged
34 gaps are identified, providing recommendations for future research.

35
36
37 **Keywords:** Natural gas pipelines; fragility; seismic intensity measures; transient ground
38 deformations; steel pipelines

1 **1. Introduction**

2 Natural gas (NG) holds a significant share in the global energy market, whilst projections for
3 the next two to three decades indicate an increasing dependence of the global energy demand
4 on this fossil fuel (International Energy Agency, 2015). NG is most commonly distributed from
5 wells to end-users, through extensive onshore networks of buried pipelines, made almost
6 exclusively of large-diameter steel pipes.

7 The increasing dependence of the energy demand of seismic prone areas on NG (e.g. south-
8 eastern Europe, China, Japan, New Zealand, west USA), gives rise to the question of the
9 seismic performance and resilience of NG networks. Earthquake-induced damages on NG and
10 fossil-fuel networks may lead to significant downtimes, which in turn may result in high direct
11 and indirect economic losses, not only for the affected area and state, but also at trans-national
12 level. Moreover, severe damages may trigger ignition or explosions with life-threatening
13 consequences and significant effects on the environment. For instance, the rupture of an oil
14 pipeline near the Santa Clara River in Colorado, USA, during the 1994 Northridge earthquake,
15 caused a large oil spill, with approximately 5 miles of pipeline empty to the ground and into
16 the river (Leville et al., 1995). The above aspects highlight the importance of simple, yet
17 efficient, seismic analysis and vulnerability assessment methods, to be used for the design of
18 new NG networks and the evaluation of the resilience of existing networks, as well as for the
19 post-earthquake management of the seismic risk through rapid and rational evaluation of
20 damages on existing networks. However, the seismic structural assessment of this type of
21 lifelines is not a straightforward task. The structural characteristics of the pipeline segments
22 (e.g. material type and strength, diameter, wall thickness, coating smoothness), the existence
23 and quality of the connections (i.e. between the pipeline segments or between the pipeline and
24 other network elements), the corrosion state and the operational pressure of the pipeline, as
25 well as the significant variations of the geomorphologic and geotechnical conditions and the
26 seismic hazard along the pipeline length, are among the parameters that may affect
27 significantly the seismic behaviour and vulnerability of NG networks (O'Rourke M.J. and Liu,
28 1999).

29 In practice, the seismic risk assessment of pipelines is mainly performed, by implementing
30 empirical fragility relations, constructed on the basis of observations of the behaviour of buried
31 pipelines during past earthquakes. A limited number of analytical fragility curves that compute
32 probabilities of failure in the 'classical sense' have also been proposed, recently (Lee et al.,
33 2016; Jahangiri and Shakid, 2018). Based on the above considerations, the main objective of
34 this two-part review paper is to critically revisit available tools for the seismic vulnerability
35 assessment of buried NG pipelines. The discussion focuses on the vulnerability of steel NG
36 pipelines subjected to transient ground deformations due to seismic wave propagation, which
37 contrary to common belief may induce non-negligible strains on the pipeline, particularly in
38 cases where the pipeline is crossing highly heterogeneous soil sites. In this part of the paper a
39 thorough critical review of available fragility relations for the vulnerability assessment of

1 buried pipelines is presented. Particular emphasis is placed on the efficiency of implemented
2 seismic intensity measures to be evaluated or measured in the field and, more importantly, to
3 correlate with observed structural damages on NG pipelines. In the second part of this paper, a
4 thorough review of alternative methods for the analytical evaluation of the vulnerability of
5 steel NG pipelines is presented, focusing on the assessment against buckling failure modes due
6 to seismically-induced transient ground deformations, which constitute a critical damage mode
7 for this infrastructure. Additionally, a new methodological approach for this assessment is
8 presented. The paper highlights the recent advancements in the field, reports gaps and
9 challenges, which call for further investigation, and provides means for an efficient assessment
10 of steel NG pipelines against seismically-induced buckling failure modes. It is worth noticing
11 that seismic wave propagation may trigger liquefaction phenomena to liquefiable soil sites,
12 which may lead to significant permanent soil deformations imposed on the pipelines. These
13 effects are out of the scope of the present study.
14

15 **2. Seismic performance and critical failure modes of buried NG pipelines**

16 Contrary to above ground structures, the seismic response of which is directly related to the
17 inertial response of the structure itself, the seismic response of embedded structures, including
18 buried pipelines, is dominated by the kinematic response of the surrounding ground (O'Rourke
19 M.J. and Liu, 1999; Hashash et al., 2001; Scandella, 2007). Post-earthquake observations have
20 demonstrated that seismically-induced ground deformations may induce extensive damages on
21 buried pipelines. More specifically, buried steel NG pipelines were found to be vulnerable to
22 permanent ground deformations associated with seismically-induced ground failures, i.e. fault
23 movements, landslides, liquefaction-induced settlements or uplifting and lateral spreading
24 (O'Rourke M.J. and Liu, 1999). Although to a lesser extent, transient ground deformations,
25 induced by seismic wave propagation, have also contributed to steel pipelines damage
26 (Housner and Jennings, 1972; O'Rourke T.D. and Palmer, 1994; O'Rourke M.J., 2009). An
27 increasing seismic vulnerability of NG pipelines was actually reported on steel pipelines that
28 were previously weakened by corrosion or poor quality welds (EERI, 1986; Gehl et al., 2014).
29 Permanent ground deformations commonly induce a higher straining on the steel pipelines,
30 compared to transient ground deformations; therefore, most research efforts have been mainly
31 focused on this seismic hazard (Karamitros et al., 2007; Vazouras et al., 2010; Vazouras et al.,
32 2012; Kouretzis et al., 2014; Vazouras et al., 2015; Vazouras et al., 2016; Karamitros et al.,
33 2016; Melissianos et al., 2017a, 2017b, 2017c; Demirci et al., 2018; Sarvanis et al., 2018;
34 Tsatsis et al. 2018, among many others). However, statistically it is more likely for a pipeline
35 to be subjected to transient ground deformations rather than seismically induced permanent
36 ground deformations. Additionally, studies have demonstrated that pipelines embedded in
37 heterogeneous sites and/or subjected to asynchronous ground seismic motions are likely to be
38 affected by appreciable deformations and strains due to transient ground deformations, which

1 in turn may lead to damages on the pipeline (Psyrras and Sextos, 2018; Psyrras et al., 2019).
2 Along these lines, this study focuses on the transient ground deformation effects.
3 A critical step in developing adequate tools for the seismic analysis, design and vulnerability
4 assessment of NG pipelines under transient ground deformation effects is to identify the
5 mechanisms that lead to failures on this infrastructure. The existence of joints and their
6 characteristics were found to affect significantly the seismic performance of pipelines,
7 generally leading to diverse damage modes on them during past earthquakes. On this basis,
8 pipelines are commonly classified as continuous or segmented (O'Rourke M.J. and Liu, 1999).
9 In the former case, pipeline segments are assembled by means of welding (e.g. welded, flanged
10 or fused joints), with the welds being at least as strong as the pipe segments. On the contrary,
11 mechanical joints are implemented for segmented pipes (e.g. coupled joints or bell and spigot
12 joints), which generally constitute the weak points of the pipeline. Continuous pipelines are
13 commonly preferred in NG networks. Supra-regional transmission networks are almost
14 exclusively made of large diameter steel pipelines, whilst for local distribution networks, steel,
15 PVC or polyethylene pipelines of small diameters are commonly used.
16 Under certain circumstances, transient ground deformation may trigger diverse damage modes
17 on continuous buried NG pipelines, including (i) shell-mode or local buckling, (ii) beam-mode
18 buckling, (iii) pure tensile rupture, (iv) flexural bending failure and (v) excessive ovaling
19 deformation of the section (O'Rourke M.J. and Liu, 1999).
20 *Shell-mode or local buckling* is associated with the loss of stability caused by compressive or
21 bending loading on the pipe. Commonly, NG networks are made of high strength steel
22 pipelines (i.e. $\sigma_y > 350$ MPa) with radius over thickness ratios $R/t < 40$. For these
23 characteristics, shell mode instabilities are expected to occur in the inelastic range of response
24 (Kyriakides and Korona, 2007). In particular, with increasing axial or bending loading on the
25 pipeline, strains begin to localize at 'critical sections' of the pipeline. Subsequently, the axial
26 stiffness of the pipe gradually decreases and wall wrinkles begin to develop at these sections,
27 followed by a limit load instability or a secondary, usually non-axisymmetric, bifurcation. The
28 highly localized strains and deformations may lead to wall tearing and hence gas leakage.
29 Imperfections of the pipelines, such as initial deviations of the walls of the pipeline from the
30 perfect geometry, may affect significantly the nonlinear load-displacement path (Kyriakides
31 and Korona, 2007). This failure mode, which has been observed on steel buried pipelines
32 during past earthquakes (Housner and Jennings, 1972; O'Rourke M.J., 2009), is more likely to
33 occur near geometric imperfections of the pipelines, or discontinuities such as girth welds and
34 elbows. *Local buckling* of buried pipelines has been a subject of early and recent studies (e.g.
35 Chen et al., 1980; Lee et al., 1984; Yun and Kyriakides, 1990; Psyrras et al., 2019) and is
36 further examined in the second part of this paper.
37 *Beam-mode or 'upheaval' buckling* leads to an upward bending of the pipe, which in some
38 cases may even be seen as a reveal of the pipe out of the ground surface. This failure mode, which
39 is likely to occur in cases of shallow-buried pipelines with low radius over thickness (R/t)

1 ratios, resembles the Euler buckling mode of a column under high compression axial loading
2 and has been observed on steel oil, gas and water pipelines during past earthquakes
3 (McNorgan, 1989; Mitsuya et al., 2013). Beam-mode buckling rarely leads to deformations
4 localization that may cause breakages and leakages. However, it may affect the serviceability
5 of the pipeline by reducing the flow of content. Along these lines, the definition of a limit state
6 on a quantitative basis is not a straightforward task. A series of numerical and experimental
7 studies have been recently carried out to further elaborate on the upheaval buckling mode (e.g.
8 Wang et al., 2011; Mitsuya et al., 2013).

9 The burial depth and the flexural stiffness of the pipe, the existence and amplitude of initial
10 geometrical imperfections on the pipe walls, as well as the soil properties of the trench, are
11 among the parameters that may control the occurrence of a shell- over a beam-mode buckling
12 failure mode on a steel pipeline (Yun and Kyriakides, 1990). However, it is quite common the
13 above failure modes to interact. Investigating this interaction, Meyersohn and O'Rourke T.D.
14 (1991) proposed a critical trench depth for buried steel pipelines that govern which failure
15 mode is preceded. They also suggested that a minimum cover depth of 0.5-1.0 m suffices to
16 prevent a beam-mode buckling.

17 Under excessive tensile axial loading, steel NG pipelines may be subjected to significant
18 plastic longitudinal strains, which in turn may lead to *tensile rupture or tensile fracture*.
19 Tensile failures rarely occur in steel pipelines with butt arc welds. On the contrary, they were
20 observed in gas-welded slip joint pipelines during the 1994 Northridge earthquake (O'Rourke
21 T.D. and O'Rourke M.J., 1995). Generally, X-grade steel pipelines, which are commonly used
22 in NG networks, may reach ultimate tensile strains of the order of 20 %. These tensile strain
23 limits are extracted from tension tests on strip specimens of base steel material, far away from
24 welds. However, imperfections associated with the welding process are expected to reduce the
25 ductility of steel pipelines. In an effort to account indirectly for the reduced ductility capacity
26 of the welded pipe weakest locations, i.e. girth welds, as well as for wall imperfections, lower
27 limits of the order of 2 - 4 %, are commonly adopted in the design practice for steel NG
28 networks (e.g. JGA, 2000; EN 1998-4, CEN 2006), while other studies propose even less limit
29 strains, of the order of 0.5 %, e.g. (Gantes and Bouckovalas, 2013). In any case, the
30 identification of the actual ultimate strain is of great importance for the accurate evaluation of
31 the response of steel pipelines under compressive axial loading, since work hardening is found
32 to affect the critical buckling load of the pipe.

33 Although theoretically it may occur, *flexural failures* of steel pipelines, associated to excessive
34 bending, are rarely expected on buried NG pipelines, owing to the high ductile steel grades
35 used. However, excessive bending may lead to beam buckling failures or ovalization of the
36 pipeline, depending on the radius over wall thickness (R/t) ratio of the pipe.

37 Large radial deformations, associated with significant bending forces, may lead to a flattening
38 of the circular cross section of a pipe in an oval-like shape, a response pattern that is also know
39 as the *Brazier effect* (Brazier, 1927). This deformation pattern is not expected to affect the

1 structural integrity of the pipeline; however, it may reduce the flowing capacity. An
2 ovalization limit, i.e. $\Delta d/D = 0.15$, has been proposed by Gresnigt (1986), prescribing the
3 change of pipe diameter Δd over the nominal diameter of the pipe D .

4 Clearly, distinct failure modes may have different consequences on the structural integrity and
5 serviceability of NG networks. Understanding the main response mechanisms behind the
6 identified failure modes, on the basis of rigorous experimental and numerical studies, may
7 contribute towards a reliable definition and quantification of limit states for NG steel pipelines.

9 **3. Fragility relations for the assessment of buried pipelines under** 10 **seismically-induced ground transient deformations**

11 **3.1 Steps in quantitative risk assessment of NG networks**

12 Aleatory and epistemic uncertainties play a vital role in earthquake engineering, as they
13 propagate through all the stages of analysis and assessment. The rapid evolving of the
14 computational capabilities, in addition to our increasing understanding of these inherent
15 uncertainties on the seismic response and vulnerability of civil infrastructure, have led to a
16 shifting from conventional deterministic analysis procedures to probabilistic risk assessment
17 concepts. On this basis, the quantitative risk assessment of a NG network should involve the
18 following critical steps (Honegger and Wijewickreme, 2013): (i) definition of the
19 characteristics of elements at risk (e.g. pipeline dimensions and steel grade, trench soil
20 properties) and the target performance and acceptable levels of risk, (ii) determination of the
21 expected seismic hazards and of their likelihood of occurrence, accounting for the associated
22 uncertainties, employing probabilistic methods, (iii) assessment of vulnerability of the
23 elements at risk (e.g. pipelines) under the expected seismic hazards (e.g. ground transient
24 deformations on buried NG pipelines), and (iv) evaluation of the probabilities of occurrence of
25 consequences associated with predefined damage states (e.g. Omidvar et al. 2013; Jahangiri
26 and Shakid, 2018). The third step of the above procedure is commonly applied in practice,
27 employing fragility relations defined for the elements at risk; in the case examined herein, the
28 NG pipelines.

29 Contemporary standards and guidelines (e.g. ALA, 2001; JGA, 2004; EN1998-4, CEN 2006)
30 provide some specifications for the seismic design of buried pipelines. However, only ALA
31 (2001) provides guidelines for the seismic vulnerability assessment of buried steel pipelines,
32 referring mainly to water-supply steel pipelines. In this context, available fragility relations,
33 referring to other typologies of buried pipelines, constitute the basis for the assessment of NG
34 pipelines (Gehl et al., 2014).

35 Generally, the seismic fragility of any element at risk can be determined as the conditional
36 probability that the response reaches or exceeds a structural limit state (LS), for a given seismic
37 intensity measure (IM). Limit states do not necessarily refer to collapse or total failure but
38

1 instead are related to predefined levels of damage state. *Fragility relations* or *curves* are used
 2 to prescribe the probability that the induced seismic demand D is equal or higher than the
 3 corresponding to a predefined limit state structural capacity C , for a given seismic IM , i.e.

$$4 \quad \text{Fragility} = P[D \geq C | IM] \quad (1)$$

5 A number of approaches may be used to develop fragility curves, which can be grouped under
 6 empirical, expert-judgement-based analytical and hybrid (Rossetto and Elnashi, 2003; Elnashai
 7 and Di Sarno, 2015; Jalayer et al., 2017; Bakalis and Vamvatsikos, 2018). The definition of the
 8 structural limit states should be based on an adequate *Engineering Demand Parameter (EDP)*,
 9 describing the response of the element at risk; the pipeline in the particular case. It is clear that
 10 both the definitions of the *EDP* and the *IM* are of prior importance for the development of
 11 adequate fragility curves.

13 3.2 Empirical fragility curves for buried pipelines

14 A variety of probabilistic empirical fragility relations have been proposed over the last 40 years
 15 for buried pipelines, based on post-earthquake observations of their response under
 16 seismically-induced permanent or transient ground deformations. The majority of these
 17 relations provide correlations between the pipeline *repair rate*, RR , i.e. the number of pipe
 18 repairs per unit of pipeline length, and a selected seismic IM , and are commonly expressed in
 19 either linear or power law forms (ALA, 2001), i.e.:

$$20 \quad RR(n^{\circ} \text{repairs} / km) = a \times IM \text{ or } RR(n^{\circ} \text{repairs} / km) = a \times IM^b \quad (2)$$

21 The parameters a and b are defined on the basis of a regression analysis of available post-
 22 earthquake damage reports of buried pipelines. It is worth noticing that the following terms
 23 have been used in relevant studies, instead of repair rate: *damage rate*, *damage ratio* or *failure*
 24 *rate*, all describing the number of pipe repairs per unit of pipeline length (Piccinelli and
 25 Krausmann, 2013). Having estimated the RR , the probability to have a total number of n
 26 damages (i.e. leaks or breaks) and repairs for a pipeline track of length L is given via a Poisson
 27 distribution, as follows (Gehl et al., 2014):

$$28 \quad P(N = n) = \frac{(RR \times L)^n}{n!} \times e^{-RR \times L} \quad (3)$$

29 The probability of a pipe failure may then be computed as:

$$30 \quad P_f = 1 - P(N = 0) = 1 - e^{-RR \times L} \quad (4)$$

31 assuming that the pipe fails when at least one damage has been occurred along its length.

32 An overview of available empirical fragility relations for buried pipelines, subjected to
 33 seismically-induced transient ground deformations, is presented in the ensuing, in
 34 chronological order, without being restricted to NG pipelines.

35 Katayama et al. (1975) presented the first charts of seismically-induced damages on brittle
 36 buried pipes, using data from six earthquakes in Japan, USA and Nicaragua. The study did not

1 account for the pipe material, diameter and joint characteristics; however, it considered the
2 effect of soil conditions on the reported damage. The seismic hazard intensity was expressed in
3 terms of peak ground acceleration (*PGA*).

4 A few years later, Isoyama and Katayama (1982) presented a *PGA*-based fragility relation
5 based on damages on cast iron pipelines reported during the 1971 San Fernando earthquake.
6 Eguchi (1983) developed fragility functions for welded steel, asbestos cement and cast iron
7 pipes, using observations from four earthquakes in USA and employing the Mercalli Modified
8 Intensity (*MMI*) as seismic *IM*. This study constitutes the first case, where pipe damages
9 caused by seismically-induced transient ground deformations and permanent ground
10 deformations were disaggregated. Barenberg (1988) proposed fragility curves for buried cast
11 iron pipes based on damage reports from three earthquakes in USA, introducing for the first
12 time the peak ground velocity (*PGV*) as seismic *IM*.

13 Ballentine et al. (1990) presented a series of *MMI*-based fragility functions for water steel
14 pipelines, using observations from six earthquakes in USA. Later studies also developed *MMI*-
15 based fragility relations for various typologies of pipelines (Eguchi, 1991; O'Rourke T.D. et
16 al., 1991) on the basis of recorded damages in USA. The Technical Council on Lifeline
17 Earthquake Engineering of the American Society of Civil Engineers (ASCE-TCLEE, 1991)
18 proposed *PGA*-based fragility relations, reanalyzing damage data on water-supply systems
19 from previous studies (Katayama et al., 1975). *PGA*-based fragility relations were also
20 proposed by Hamada (1991) and O'Rourke T.D. et al. (1991) employing damage reports from
21 earthquakes in the USA and Japan.

22 A *PGV*-based fragility relation was proposed by O'Rourke M.J. and Ayala (1993) for brittle
23 cast iron pipelines, using damage reports from earthquakes in USA and Japan. The study
24 highlighted the effect of corrosion state of the pipelines on their seismic vulnerability. The
25 proposed fragility relation was later adopted by FEMA in the HAZUS methodology (NIBS,
26 2004) for the evaluation of seismic vulnerability of pipes subjected to seismically-induced
27 transient ground deformations. A reduction factor, i.e. 0.3, was introduced on the initial
28 fragility relation in order this to be applicable for ductile pipelines, such as steel NG pipelines,
29 as well. It is worth noticing that the particular fragility function does not account for the critical
30 effect of the size of the pipe on its seismic vulnerability.

31 Reanalyzing the pipeline damage reports used by O'Rourke M.J. and Ayala (1993), Eidinger et
32 al. (1995) developed a new *PGV*-based fragility relation. The study that was further described
33 in Eidinger et al. (1998) examined the effect of a number of salient parameters on the seismic
34 vulnerability of buried pipelines, i.e. the pipe diameter, material, joint type, coating, the trench-
35 soil conditions and the date of installation. The effects of the above parameters were
36 considered in the proposed fragility relation through the introduction of a modification factor
37 K_I and a *quality index*, the latter related with the confidence of the available empirical data set.
38 Reanalyzing damage reports from previous studies (Katayama et al., 1975; TCLEE-ASCE,

1 1991; Hamada, 1991; O'Rourke et al., 1991), Hwang and Lin (1997) developed a new *PGA*-
2 based fragility function for buried pipelines.

3 Trifunac and Todorovska (1997) developed fragility relations for water-supply pipelines, using
4 damage reports from the 1994 Northridge earthquake in California, USA. The fragility
5 relations were plotted on basis of damage rates per square km of land area, while the severity
6 of the ground motion was described employing the peak soil shear strain (γ_{max}), computed near
7 the soil surface, as: $\gamma_{max} = PGV/V_{s,30}$, where $V_{s,30}$ is the average shear wave velocity of the top
8 30 m of the soil deposit.

9 O'Rourke T.D. et al. (1998) implemented a detailed geographic information system (GIS) to
10 examine for a first time the efficiency of various seismic *IMs* to correlate with observed
11 damage rates of pipelines. The study employed reported damages on cast iron pipelines of the
12 water-supply system of California, induced by the 1994 Northridge earthquake. From the
13 seismic *IMs* that were considered in the study, i.e. *MMI*, *PGA*, *PGV*, spectral acceleration *SA*,
14 spectral intensity *SI*, and Arias intensity I_a , *PGV* was found to be more efficient in correlating
15 with observed damages. A year later, a new fragility relation was proposed by O'Rourke T.D.
16 and Jeon (1999) for cast iron pipes using data from the same earthquake in California, USA. A
17 new metric, i.e. the *scaled velocity*, was used seismic *IM*, defined by normalizing *PGV* by the
18 diameter of the pipe, so as to account for the effect of the pipe size on its seismic vulnerability.
19 Reported damages on the water-supply network of Kobe during the destructive 1995
20 Hyogoken-Nambu earthquake were exploited by Isoyama et al. (2000) to develop *PGA*- and
21 *PGV*-based fragility relations for steel pipes. A series of correction coefficients were proposed
22 to account for the effects of pipe material and diameter, trench-soil conditions, as well as soil
23 liquefaction occurrence, on the seismic vulnerability of pipelines.

24 In 2001 the American Lifelines Alliance (ALA, 2001) published detailed guidelines for the
25 seismic assessment of water-supply networks, which included *PGV*-based fragility relations for
26 buried pipelines subjected to seismically-induced transient ground deformations. The relations
27 that were defined using more than 80 damage reports from diverse seismic events in USA, are
28 provided as 'backbone' curves that may properly be adjusted through correction parameters, so
29 as to account for the effects of salient parameters, such as the pipe material and diameter and
30 the joint characteristics, on the seismic vulnerability of the pipe. It is worth noticing that the
31 relations were derived from very scattered damage data, which refer mainly to brittle pipes
32 made of cast iron or asbestos cement.

33 Chen et al. (2002) examined the response of NG and water-supply pipelines of the Taichung
34 City during the 1999 Chi-Chi earthquake and developed fragility relations for various pipe
35 diameters and materials (polyethylene, steel, cast iron) using relevant damage reports. A
36 variety of relations were actually developed using *PGA*, *PGV* and spectrum intensity *SI*, as
37 seismic *IMs*. Interestingly, the researchers noticed a better correlation of damage rates with
38 *PGA*, while *PGV* was found to be the worst damage indicator. However, their relations and

1 relevant observations were based on rather limited damage reports. Pineda and Ordaz (2003)
2 developed *PGV*-based fragility functions for brittle cast iron and asbestos cement water pipes
3 based on the observed behaviour of the water-supply system of Mexico City during the 1985
4 earthquake.

5 Reanalysing the fragility relations proposed by O'Rourke M.J. and Ayala (1993) and Jeon and
6 O'Rourke T.D. (1999), O'Rourke M.J. and Deyoe (2004) revealed differences on their
7 predictions, which were attributed to various parameters, including the seismic wave type that
8 dominated the ground-pipeline system response in each reported case, the corrosion state of the
9 pipe and the low statistical reliability of some of the used data. Classifying the statistical
10 reliable damage reports and making reasonable assumptions regarding the dominant seismic
11 wave in each case, the researchers proposed *PGV*-based relations in a first effort to account for
12 the type of the controlling seismic wave. The main assumption for the development of the
13 latter curves was that body shear waves, i.e. *S*-waves, control the response and damage
14 potential of pipelines that are located near the seismic source, whereas surface Rayleigh waves,
15 i.e. *R*-waves, govern the pipeline response in far-field sites. Finally, assuming an apparent
16 velocity of 500 m/s and 3000 m/s for the *R*-waves and the *S*-waves, respectively, the
17 researchers computed the Peak Ground Strain (ϵ_g) (see Section 4.2.4) for each damage case and
18 developed ϵ_g -based fragility relations. Generally, a more consistent correlation between
19 reported damages on pipelines and Peak Ground Strain (ϵ_g) was reported by the researchers
20 compared to *PGV*.

21 Reanalyzing pipeline damage reports from the study of O'Rourke T.D. et al. (1998), Jeon and
22 O'Rourke T.D. (2005) proposed *PGV*-based fragility functions for various types of pipelines,
23 i.e. welded steel, cast iron, ductile iron and asbestos cement pipelines.

24 The 1985 Michoacán earthquake in Mexico City was used as a case study by Pineda-Porras
25 and Ordaz (2007) to propose a fragility relation for the seismic vulnerability assessment of
26 brittle water-supply pipelines embedded in soft soil, introducing a new vector seismic *IM*, i.e.
27 PGV^2/PGA . The proposed *IM* was claimed to correlate better with observed damages compared
28 to *PGV*, particularly in cases of soft soils. Two years later, an updated ϵ_g -based fragility
29 function for buried segmented pipelines was presented by O'Rourke M.J. (2009).

30 O'Rourke T.D. et al. (2014) examined the response of buried water-supply, wastewater and
31 NG pipeline networks of Christchurch, New Zealand, during the 2011 Canterbury earthquake
32 sequence. Using damage reports of brittle water-supply pipelines, they developed *PGV*-based
33 fragility relations, with *PGV* being defined as the geometric mean peak ground velocity. The
34 study highlighted the very good performance of the NG distribution network, which consisted
35 mainly of very ductile high-density polyethylene pipes. Extending his previous study
36 (O'Rourke M.J., 2009) with observed damage reports from the 1999 Kocaeli earthquake in
37 Turkey, O'Rourke M.J. (2015) proposed a new ϵ_g -based fragility relation.

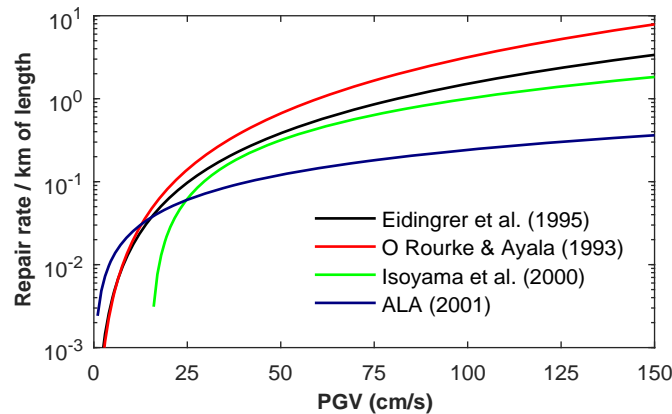
38 A summary of commonly used empirical fragility relations for buried pipelines, subjected to
39 seismically-induced transient ground deformations, is provided in Table 1.

1 **Table 1.** Empirical fragility functions for buried pipelines subjected to transient ground deformations
 2 due to wave propagation.

Reference	Relation	Applicability and notes
Katayama et al. (1975)	$RR = 10^{b+6.39 \log PGA}$	valid mainly for cast iron pipes, $b=3.65$ for average conditions
Isoyama and Katayama (1982)	$RR = 1.698 \times 10^{-16} \times PGA^{6.06}$	valid mainly for cast iron pipes
O'Rourke M.J. and Ayala (1993)	$RR = (PGV / 50)^{2.67}$	valid mainly for cast iron pipes
O'Rourke T.D. et al. (1998)	$RR = 10^{1.25 \times \log PGA - 0.63}$	valid mainly for cast iron pipes
Eidinger (1998)	$RR = K_1 \times 0.0001658 \times PGV^{1.98}$	valid for arc welded steel pipes, K_1 is a correction factor to account for particular characteristics of the examined pipeline
O'Rourke T.D. and Jeon (1999)	$RR = 0.00109 \times PGV^{1.22}$	valid for cast iron pipes
Isoyama et al. (2000)	$RR = 2.88 \times 10^{-6} \times (PGA - 100)^{1.97}$	valid mainly for cast iron pipes
Isoyama et al. (2000)	$RR = 3.11 \times 10^{-3} \times (PGV - 15)^{1.30}$	valid mainly for cast iron pipes
O'Rourke et al. (2001)	$RR = e^{1.55 \times \ln PGV - 8.15}$	valid mainly for cast iron pipes
American Lifelines Alliance (2001)	$RR = 0.002416 \times PGV \times K_1$	K_1 is a correction factor to account for particular characteristics of the pipeline
O'Rourke M.J. and Deyoe (2004)	$RR = 513 \times \varepsilon_g^{0.89}$	valid for segmented pipes subjected to transient ground deformations
	$RR = 724 \times \varepsilon_g^{0.92}$	valid for segmented pipes subjected to transient or permanent ground deformations
	$RR = 0.0035 \times PGV^{0.92}$	valid for pipelines subjected to S-waves
	$RR = 0.034 \times PGV^{0.92}$	valid for pipelines subjected to R-waves
O'Rourke M.J. (2009)	$RR = 190 \times \varepsilon_g^{1.12}$	valid for segmental pipes
O'Rourke T.D. et al. (2014)	$RR = 10^{-4.52} \times PGV^{2.38}$	valid for cast iron pipes
O'Rourke T.D. et al. (2014)	$RR = 0.41 + 0.0839 \times \varepsilon_g$	valid for cast iron pipes
O'Rourke M.J. et al. (2015)	$RR = 2951 \times \varepsilon_g^{1.16}$	valid for segmental pipes

3
 4 Based on the above overview, it is evident that most empirical fragility relations have been
 5 proposed for water-supply pipeline networks. In this context, the implementation of these
 6 functions in steel NG pipelines, the dimensions and the operational pressures of which, are
 7 quite distinct, might be questionable. Based on comparisons of the predictions of available
 8 empirical fragility relations with reported damages on buried pipeline networks during the
 9 1999 Dutze earthquake, in Turkey, and the 2003 Lefkas earthquake, in Greece, Alexoudi
 10 (2005) and Pitilakis et al. (2005), suggested the use of the Isoyama et al. (2000) fragility
 11 relations for NG networks, while the use of ALA (2001) relations was proposed for water-
 12 supply and waste-water networks.
 13 Gehl et al. (2014) suggested that the empirical fragility relations by O'Rourke M.J. and Ayala
 14 (1993), as adopted by HAZUS (NIBS, 2004), Eidinger et al. (1995), Isoyama et al. (2000) and

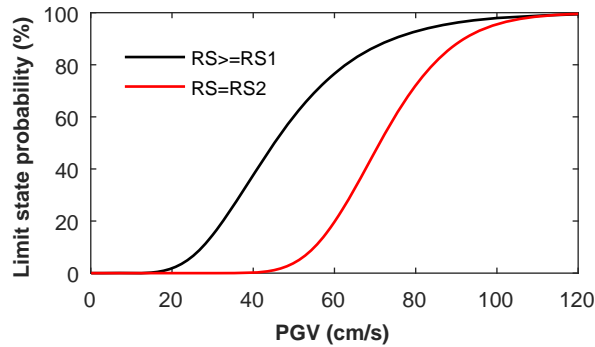
1 ALA (2001), constitute adequate candidates for the assessment of continuous ductile welded-
2 steel, PVC and HDPE pipelines that are commonly used in NG networks. The latter relations,
3 which all use PGV as seismic IM , are comparatively presented in Figure 1. O'Rourke M.J. and
4 Ayala (1993) fragility relation was defined on the basis of damage reports of cast iron pipes;
5 hence, its applicability in ductile steel NG pipes is arguable. Moreover, the relation is reported
6 to be over-conservative as the pipeline damage data on which it is based, was most probably
7 biased by the long duration ground seismic motions of the 1985 Michoacán earthquake
8 (O'Rourke, T.D., 1999; Tromans, 2004). On the other hand, the Isoyama (2000) and the ALA
9 (2001) relations offer a longer applicability range in terms of PGV values (see also *Section*
10 *4.3.2*). The former relation was proposed on the basis of damage reports in Japan; hence its
11 applicability in other sites abroad is again questionable. ALA (2001) provides a more recent
12 reference and is based on an extended database of damage reports from USA and Japan. It is
13 worth noticing the available empirical fragility relations do not consider polyethylene
14 pipelines. As mentioned above, these pipelines revealed a very good performance during the
15 2011 Canterbury earthquake sequence owing to their high ductility (O'Rourke et al., 2014).
16



17
18 **Figure 1.** Comparison of empirical fragility relations for buried pipelines, which could potentially be
19 used in the seismic vulnerability assessment of NG networks (after Gehl et al., 2014).
20

21 Empirical fragility curves for the vulnerability assessment of continuous steel-welded NG
22 pipelines subjected to seismically-induced transient ground deformations, in the classical
23 definition of Equation 1, i.e. by computing probabilities of exceedance of particular
24 performance levels for a given level of seismic intensity, were proposed for the first time by
25 Lanzano et al. (2013). The researchers proposed three discrete damage states (DS) that were
26 associated with corresponding risk states (RS). The former states describe the type and level of
27 structural damage on the pipeline (i.e. $DS0$: slight damages, $DS1$: significant damages, $DS2$:
28 severe damages), whereas the latter are defined based on the potential consequences (i.e. $RS0$:
29 no losses - null hazard, $RS1$: limited losses - low hazard, $RS2$: non-negligible losses - high
30 hazard). Based on the above definitions, PGV -based relations were established by fitting well-
31 documented damage reports of continuous steel pipelines during past earthquakes, with a

1 lognormal cumulative distribution function (Figure 2). This study was then extended in
2 Lanzano et al. (2014) to develop fragility functions for NG pipelines subjected to seismically-
3 induced ground deformations. The list of damage reports used to construct the fragility
4 functions were presented in detail in Lanzano et al. (2014; 2015).



6
7 **Figure 2.** Fragility curves for continuous buried NG steel pipelines developed by Lanzano et al. (2013)
8 on the basis of reports from actual damages during past earthquakes.

9 10 **3.3 Analytical fragility curves for buried NG pipelines**

11 A few recent studies have employed numerical methodologies to develop analytical fragility
12 curves, in the sense of Equation 1. Lee et al. (2016) presented a set of analytical *PGA*-based
13 fragility curves for a buried steel NG pipeline with a diameter of 762 mm (30 in) and a wall
14 thickness of 17.5 mm (i.e. radius over thickness ratio $R/t = 21.8$). The fragility curves were
15 developed on the basis of an incremental dynamic analysis (IDA), using simplified numerical
16 models to account for the soil-pipe interaction effects. In particular, the analyses were
17 conducted using the finite element code ZeusNL, with the pipeline being simulated with
18 inelastic cubic line elements and the soil compliance being modelled by means of discrete
19 nonlinear springs in the three translational directions (axial, transverse and vertical). The soil
20 springs were validated using the relevant regulations of ALA (2001). The total length of the
21 models was set equal to 1.2 km, whilst various assumptions were made with regard to the
22 burial depth of the pipeline, the soil properties of the trench (i.e. homogeneous, heterogeneous
23 soils along the pipeline axis) and the boundary conditions at the end-sides of the pipeline (i.e.
24 fixed or pinned conditions). Unfortunately, only the strength properties of the selected soil
25 deposits were given, while no information regarding the soil stiffness was provided in the
26 relevant paper. The majority of analyses were conducted assuming a straight pipeline, while a
27 number of analyses were also carried out, by assuming over- or sag-bends on the pipeline. The
28 latter are commonly used in crossings of NG pipelines with rivers or existing civil
29 infrastructure. The maximum axial strain, which was computed at critical sections of the
30 pipeline, such as the end-boundaries and the bends (when existed), was used as *EDP* for the
31 construction of the fragility curves. It is inferred from the paper that no desegregation between
32 compressive or tensional axial strains was made by the researchers. For a uniform soil deposit,

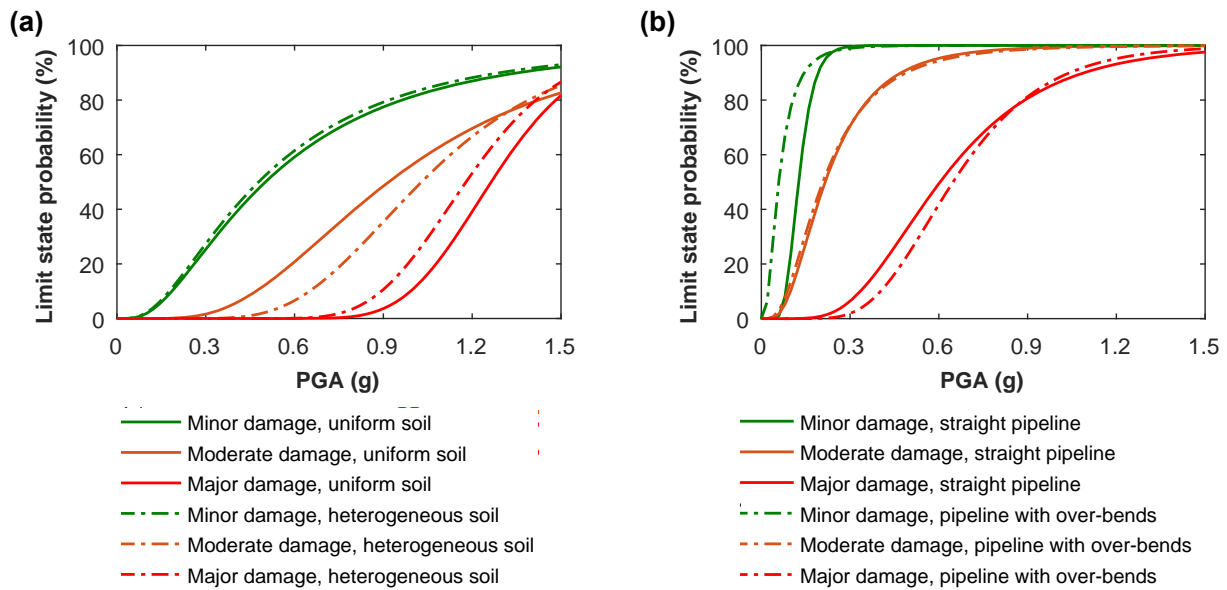
1 the strains on the pipe are indeed expected on the sections that were selected by the
 2 researchers. However, for heterogeneous soil deposits, high pipe straining is expected at the
 3 sections where the soil properties are changing. Three limit states, i.e. minor, moderate and
 4 major damages, were defined as fractions of the steel material yield strain (Table 2), following
 5 Shinozuka et al. (1979). Considering the high ductility of the steel grades used in NG
 6 networks, this definition might be considered as quite conservative. The analyses were carried
 7 out for 12 recorded ground seismic motions, scaled to a range of earthquake intensities, i.e. 0.1
 8 g to 1.5 g. An increasing pipe straining was reported with a decreasing burial depth of the
 9 pipeline. Additionally, the seismic vulnerability of the examined pipe was increased when
 10 looser soil deposits were considered, while it was found to be sensitive to the boundary
 11 conditions adopted at the end-sides.

12
 13 **Table 2.** Limit states for NG steel pipelines as adopted by Lee et al. (2016). ε_p is the maximum axial
 14 strain induced on the pipeline during ground seismic shaking, while ε_y is the yield strain of pipeline
 15 steel material.

Damage state	Description
Minor damage	$\varepsilon_p \leq 0.7 \times \varepsilon_y$
Moderate damage	$0.7 \times \varepsilon_y \leq \varepsilon_p \leq \varepsilon_y$
Major damage	$\varepsilon_p > \varepsilon_y$

16
 17
 18 Figure 3 illustrates representative analytical fragility curves from this study, highlighting the
 19 effects of soil heterogeneities along the pipeline axis (Figure 3a), as well as of the existence of
 20 bends (Figure 3b) on the seismic vulnerability of the examined pipeline. A slightly higher
 21 vulnerability is reported for the minor and major damage states, when the pipe is considered to
 22 be embedded in a heterogeneous soil deposit, while the reverse holds for the moderate damage
 23 state. Interestingly, the effect of pipe bends on the seismic vulnerability of the examined pipe
 24 was found to be quite reduced. The latter results may have been biased, at least to some extent,
 25 by the simplified simulation of the soil compliance and the pipeline itself.

26



1 **Figure 3.** Effects of (a) trench soil properties, (b) pipeline bends on analytical fragility curves
2 developed by Lee et al. (2016), referring to a 762 mm diameter continuous buried NG steel pipeline
3 under transient ground deformations.
4

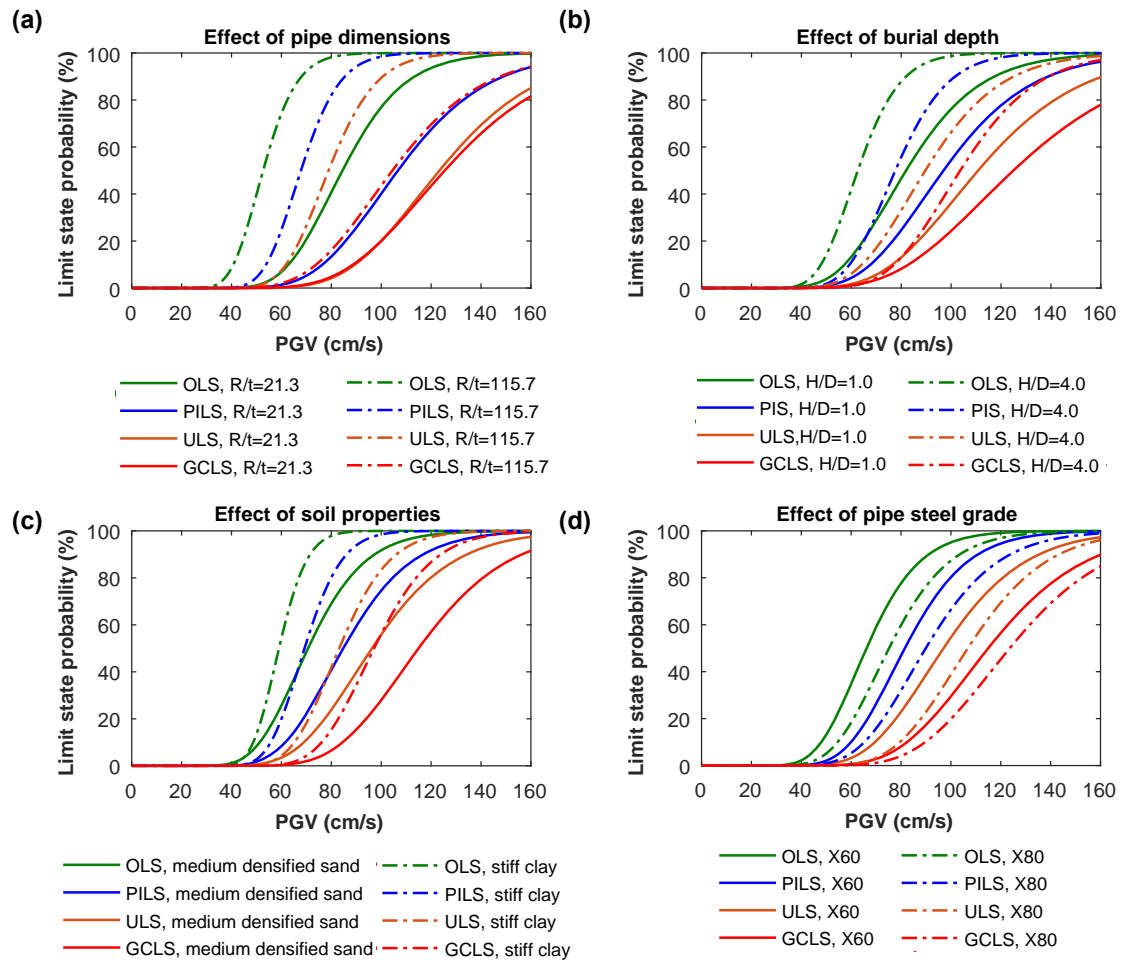
5
6 In a more detailed study, Jahangiri and Shakib (2018) investigated the seismic vulnerability of
7 buried steel NG pipelines, proposing a series of analytical *PGV*-based fragility curves. The
8 fragility curves were developed on the basis of an IDA, implementing numerical models of the
9 examined soil-pipe configurations developed in the finite element code OpenSees. In
10 particular, the examined pipes were modelled using 3D beam elements with fiber sections in
11 the circumferential and radial directions, obeying a nonlinear Ramberg-Osgood material
12 model. The soil compliance was simulated by means of nonlinear spring elements acting in
13 axial, transverse and vertical directions, as per ALA (2001) regulations. Additionally, discrete
14 damper elements were implemented, defined following Hindy and Novak (1979). The length of
15 the soil-pipe models was set equal to 1 km, while nonlinear springs were introduced at both
16 end-sides of the examined systems, in order to account for the infinite length of the pipeline,
17 following Liu et al. (2004). Salient parameters that affect the seismic response and
18 vulnerability of NG pipelines, such as the pipe dimensions, burial depth and steel grade, and
19 the soil properties of the trench, were considered. The diameter over thickness ratios (D/t) of
20 the selected pipes ranged between 21 and 116. It is worth noticing that large diameter steel
21 pipelines, commonly found in NG transmission networks (i.e. diameters $D > 800$ mm) were not
22 considered. The burial depth over diameter ratios (H/D) varied between 1 and 4, while the
23 effect of steel material grade was accounted for by considering API 5L X60, X65, X70 and
24 X80 steel pipes. The shear wave velocities of the adopted soil sites ranged between 180 m/s
25 and 360 m/s. Full dynamic time history analyses were conducted using 20 far-field records.
26 The records were appropriately scaled and applied on the examined soil-pipe systems in equal
27 *PGV* steps of 10 cm/s. The maximum axial compressive strain computed at the most critical

1 section of the pipeline was selected as *EDP*. Four limit states, corresponding to various levels
 2 of damage, were defined, as per Table 3, following the relevant references, also provided in the
 3 table. Obviously, a more rigorous definition of limit states was made herein, compared to Lee
 4 et al. (2016).

5
 6 **Table 3.** Limit states adopted Jahangiri and Shakib (2018), *t*: thickness of the pipeline, *D*: diameter of
 7 the pipeline

Limit state	Maximum allowable axial compressive strain	Description	Return period (years)	ε_c defined following
Operable Limit State (OLS)	$\varepsilon_c = \min(0.01, 0.4 \times t/D)$	Despite some minor plastic deformation, the pipeline will operate immediately after the event.	25	ALA (2001), JGA (2004), EN1998-4 CEN S(2006)
Pressure Integrity Limit State (PILS)	$\varepsilon_c = \min(0.04, 1.76 \times t/D)$	Despite some significant deformations on the pipe, no leakage of containment is taken place.	95	ALA (2001), JGA (2004), EN1998-4 CEN (2006), Mohareb (1995), Honegger et al. (2002), Bai and Bai (2014)
Ultimate Limit State (ULS)	$\varepsilon_c = \min(0.1, 4.4 \times t/D)$	A 'controllable' release of the containment of the pipeline is acceptable.	475	Bai (2001), Honegger et al. (2014), Bai and Bai (2014)
Global Collapse Limit State (GCLS)	$\varepsilon_c = \min(0.15, \varepsilon_{GDI})$	A structural collapse is reported. ε_{GDI} is the strain level obtained at global dynamic instability of the analysis, i.e. when the analysis can not converge and numerically infinite <i>EDPs</i> are computed.	2475	Zhang (2008), Nazami and Das (2010), Ahmed et al. (2011), Bai and Bai (2014)

8
 9
 10 Figure 4 illustrates representative analytical fragility curves developed within this study. More
 11 specifically, the effects of the dimensions and burial depth of the pipeline on its seismic
 12 vulnerability are highlighted in Figures 4a and 4b, respectively. The comparisons indicate an
 13 increase of the failure probabilities of NG pipelines with decreasing *D/t* ratios, as well as with
 14 increasing *H/D* ratios (i.e. with increasing burial depth). Figures 4c and 4d compare analytical
 15 fragility curves for diverse pipe-trench-soil configurations, highlighting the effects of the
 16 trench soil properties and steel grade of the pipe on the seismic vulnerability of NG pipelines.
 17 Higher failure probabilities are reported with an increasing stiffness of the surrounding ground,
 18 as well as with a reducing steel grade of the pipe. The effects of the above parameters on the
 19 axial response and vulnerability of steel pipelines are further addressed and discussed in the
 20 second part of this paper.



1
2 **Figure 4.** Comparisons of analytical fragility curves developed for buried NG steel pipelines by
3 Jahangiri and Shakib (2018).

4
5 **3.4 Critical discussion on available fragility relations for buried pipelines**

6 The majority of available fragility relations refer to cast-iron or asbestos cement segmented
7 pipelines, the seismic response of which is quite distinct compared to continuous pipelines
8 (O'Rourke M.J. and Liu, 1999). The lack of relevant damage reports and therefore of relevant
9 fragility relations for continuous pipelines has been attributed by some researchers to their
10 better performance, compared to the segmental pipelines, when subjected to seismically-
11 induced transient ground deformations. However, several studies have demonstrated that under
12 particular circumstances, transient ground deformations may result in appreciable strains on
13 continuous pipelines, which in turn may lead to damages as well (O'Rourke M.J., 2009;
14 Psyrras and Sextos, 2018; Psyrras et al., 2019).

15 The usage of *repair rate* as an *EDP* does not provide any information regarding the severity of
16 damage, as well as the type of required repair. The only available recommendation to define
17 the expected damage level on the pipeline is provided by HAZUS (NIBS, 2004) and is based
18 on the type of seismic hazard. For seismically-induced transient ground deformations, it is
19 simply proposed that leaks will appear at 80 % of the reported damages, while the less 20 %

1 will correspond to breaks. The reverse holds for seismically-induced permanent ground
2 deformations.

3 The quality and accuracy of the repair reports after a seismic event and the lack of knowledge
4 regarding the incident angle between the pipeline axis and the ray path of the seismic wave are
5 other acknowledged issues that may induce a high level of uncertainty to the empirical fragility
6 relations. The accuracy of the repair reports that constitute the basis for the development of
7 empirical fragility functions may be debatable, since these are commonly drafted after a short
8 period from the main event and under the pressure for rapid restorations. The incident angle
9 between the ray path and the pipeline axis that is expected to affect notably the pipeline
10 response and vulnerability (O'Rourke M.J. et al., 1980; Pineda-Porras and Najafi, 2010) is not
11 known and therefore its crucial effect on the empirical relations statistics is not considered.
12 Indeed, if a pipeline is oriented in parallel with the propagation of surface Rayleigh waves, the
13 expected straining that will be imposed on the pipe and the potential damages are increased
14 considerably. On the contrary, if the Rayleigh waves are propagating in the perpendicular
15 direction to the pipeline axis, no damage is expected on the pipe. Additionally, the reliability of
16 the repair ratio statistics is highly sensitive to the pipeline lengths sampled in each interval of
17 the selected seismic *IM* (O'Rourke T.D. et al., 2014).

18 The majority available empirical relations were developed on the basis of damage reports on
19 pipeline networks found in USA and Japan, whilst in southern Europe or other seismic prone
20 areas there is tremendous lack or relevant information. Among few exceptions are, the 2003
21 Lefkas earthquake, where damages were reported and examined on the water-supply network
22 of the city (Alexoudi, 2005; Pitilakis et al., 2006; Paolucci and Pitilakis, 2007), as well as the
23 reported damages on the NG network of L'Aquila during the 2009 earthquake (Esposito et al.,
24 2014). Evidently, the applicability of the empirical fragility relations is restricted to cases
25 where the network (e.g. pipe dimensions and materials, soil conditions etc), and the ground
26 motion characteristics, are similar to the relevant characteristics of the sample used to develop
27 the relations. Along these lines, a general and unconditional use of these relations might
28 introduce a significant degree of uncertainty in the seismic risk assessment of networks with
29 distinct characteristics (Psyrras and Sextos, 2018).

30 The most important drawback of empirical fragility relations is that they do not disaggregate
31 between the potential damage modes (i.e. local or beam buckling, tensile rupture and
32 ovalization for continuous pipelines). As discussed in *Section 2*, different damage modes are
33 associated with different risks and effects on the structural integrity and serviceability of the
34 pipeline. Along these lines, the efficiency of empirical fragility relations in a rapid and valid
35 post-earthquake risk assessment of existing NG networks might be highly arguable.

36 The available analytical fragility functions for NG pipelines that were developed recently refer
37 to rather limited number soil-pipe configurations and do not cover NG pipelines with diameters
38 larger than 800 mm that are commonly used in transmission NG networks. The analytical
39 fragility curves use more rigorous *EPDs* compared to the empirical fragility relations, e.g. the

1 pipeline axial compressive strain; however, the evaluation of these *EPDs*, as well as the
2 definition of limit states, associated with particular damage modes, are still open issues, which
3 call for further investigation. More importantly, the relevant numerical studies do not examine
4 thoroughly salient parameters that may affect the response and hence the vulnerability of
5 buried NG pipelines under seismically-induced transient ground deformations, such as the
6 effects of the internal operational pressure of the pipeline, the geometric imperfections of the
7 walls of the pipes and the spatial variability of the seismic ground motion along the axis of the
8 pipeline. The effects of the above parameters on the structural response and vulnerability of
9 NG pipelines are further discussed in the second part of this paper.

10 Along these lines, additional research is deemed necessary towards the development of
11 analytical fragility functions that will account for the above critical parameters and will cover a
12 wide range of soil-pipe typologies, commonly used in NG applications. One critical issue
13 towards the development of rigorous analytical fragility curves is the identification of
14 ‘adequate’ intensity measures that may efficiently be used to describe the effect of seismic
15 intensity on the vulnerability of pipelines for the identified damage modes. In the following
16 section, a critical review of the commonly used for buried pipelines seismic *IM* is made,
17 focusing on their efficiency to correlate with observed damages on pipelines, as well as to be
18 determined or measured in the field.

20 **4. Seismic intensity measures for buried pipelines**

22 **4.1 Why the selection of adequate seismic intensity measures is important?**

23 The severity of a ground seismic motion in fragility relations is expressed by means of a
24 seismic intensity measure (*IM*) (Baker and Cornell, 2005). Generally, a seismic *IM* should
25 provide information regarding various characteristics of a seismic ground motion, including its
26 amplitude, duration and frequency and energy content, which are all expected to affect the
27 seismic vulnerability of any element at risk. Available seismic *IMs* may be classified as
28 empirical or instrumental. In the former case, the severity of the seismic hazard is described by
29 means of macro-seismic intensity scales, whereas in the latter case analytical values, recorded
30 by an instrument or computed via a seismic hazard analysis, are used. The *optimum* seismic *IM*
31 should be *efficient*, in the sense that it results in reduced variability of the *EDP* for a given *IM*
32 value (Shome and Cornell, 1998) and in parallel *sufficient*, in the sense that it renders the
33 structural response conditionally independent of the earthquake magnitude (*M*), source-to-site
34 distance (*R*) and other seismological parameters (e.g. ϵ) (Luco and Cornell, 2007). An efficient
35 *IM* allows for a reduction of the number of numerical analyses and ground seismic motions that
36 are required to estimate the probability of exceedance of each value of the *EDP* for a given *IM*
37 value. On the other hand, a sufficient *IM* allows for a free selection of the seismic ground
38 motions, since the effects of seismological parameters on the prediction of the *EDP* are less
39 important. Both the efficiency and sufficiency of a seismic *IM* may rigorously be defined

1 following recently-developed analysis frameworks for the performance based design, as well as
 2 the probabilistic risk assessment of the structures (Cornell and Krawinkler, 2000; Luco and
 3 Cornell, 2007).

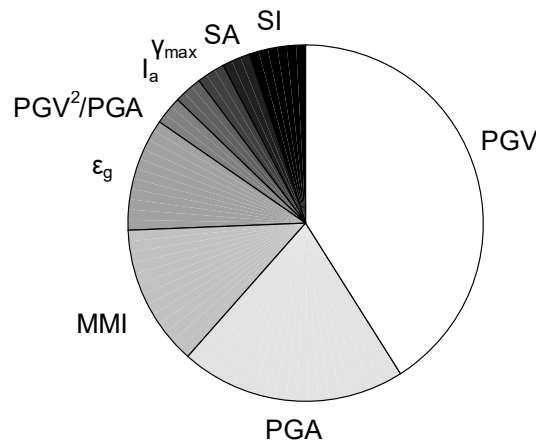
4 In particular, the Pacific Earthquake Engineering Research Center (PEER) framework allows
 5 the calculation of the loss by integrating over particular levels of the seismic hazard, the
 6 response and damage with the contributions of each of those variables weighted by their
 7 relative likelihood of occurrence. The method accounts for the uncertainties involved in all the
 8 variables and their in between relations in a mathematically rigorous formality, known as the
 9 total probability theorem:

$$\lambda[DV] = \iiint_{DM,EDP,IM} G[DV|DM] dG[DM|EDP] dG[EDP|IM] \lambda[IM] \quad (5)$$

11 where DV is the decision variable(s), e.g. fatalities due to ignitions or explosions caused by
 12 potential leakages from NG pipelines, direct or indirect monetary losses associated to
 13 downtimes of a NG network etc., DM is the damage measure(s), e.g. buckling or tensile rupture
 14 of the pipeline etc., EDP is the engineering demand parameter, e.g. the maximum compressive
 15 or tensile strain on a steel NG pipeline, and IM is the seismic intensity measure. $G(\cdot)$ stands for
 16 the complementary cumulative distribution function (CCDF) or probability of exceedance. The
 17 CCDFs that are found in Equation 5 from left to right may be evaluated from the loss, damage
 18 and response models. The term $\lambda[IM]$ may be obtained via a probabilistic seismic hazard
 19 analysis, i.e. by implementing a seismic hazard curve. Evidently, a critical step in the above
 20 analysis procedure is the development of functional relationships between the EDP and the
 21 selected seismic IM on the basis of predictions of relevant numerical analyses. Various
 22 approaches have been proposed in the literature for this purpose, including the incremental
 23 dynamic analysis (IDA) (Vamvatsikos and Cornell, 2002), the multiple-stripe analysis (Jalayer
 24 and Cornell, 2009) and the cloud analysis (Jalayer et al., 2015). The $EDP-IM$ relations
 25 developed by any of the above methods may be used to evaluate in a mathematically rigorous
 26 way the efficiency and sufficiency of any seismic IM . As stated, an efficient IM will result to
 27 reduced variability of the EDP for a given IM value. Quantifying the sufficiency of a seismic
 28 IM requires the separate regression analysis of the EDP relative to seismological parameters,
 29 e.g. the magnitude M and the epicentral distance R .

30 Other concepts and quantities, namely the *practicality*, *effectiveness*, *robustness*, *computability*
 31 *and proficiency*, have been proposed before for identifying the optimum seismic IM for
 32 buildings, bridges and above ground civil infrastructure (indicatively: Shome et al., 1998,
 33 Mackie and Stojadinovic, 2003, Baker and Cornell, 2005; Vamvatsikos and Cornell, 2005,
 34 Luco and Cornell, 2007, Padgett and DesRoshes, 2008, Yang et al., 2009, Kostinakis et al.,
 35 2015, Fotopoulou and Pitilakis, 2015, among many others). Evidently, an efficient
 36 determination of the spatial distribution of a selected seismic IM is of great importance in the
 37 assessment of an extended network (De Risi et al., 2018).

1 As indicated in *Section 3*, various seismic *IM* have been adopted in empirical and analytical
 2 fragility relations for buried pipelines, including *MMI*, *PGA*, *PGV*, ϵ_g , I_a , *SI*, as well as
 3 PGV^2/PGA . Figure 5 illustrates the proportions of the seismic *IMs* used by the available
 4 empirical and analytical fragility relations for buried pipelines. The graph follows Gehl et al.
 5 (2014), whilst being updated by recent empirical and analytical studies. Clearly, *PGV* has a
 6 dominant presence as seismic *IM* in the available functions, while *PGA*, *MMI* and ϵ_g are
 7 following. A relevant comparative discussion on the efficiency (in a general sense) of the
 8 above seismic *IMs* was made by Pineda-Porras and Najafi (2008). In a more recent study,
 9 Shakid and Jahangiri (2016) examined the efficiency and sufficiency of 18 seismic *IMs* for NG
 10 pipelines, on the basis of a numerical parametric study. More details about the latter study are
 11 provided in the ensuing. Before that a critical revisit of the seismic *IMs* used in empirical and
 12 analytical fragility relations for buried pipelines so far, as well as some elements from relevant
 13 comparative studies, are presented.



14
 15 **Figure 5.** Relative proportions of seismic *IMs* used in empirical or analytical fragility functions for
 16 buried pipelines subjected to transient ground deformations due to wave propagation.

17
 18
 19 **4.2 Critical review of seismic *IMs* used in empirical fragility relations and analytical**
 20 **fragility curves for buried pipelines**

21
 22 **4.2.1 Modified Mercalli Intensity (MMI)**

23 Modified Mercalli Intensity was used as seismic *IM* for buried pipelines in early studies
 24 (Eguchi, 1983; Ballentine et al., 1990; Eguchi, 1991; O'Rourke T.D. et al., 1991; O'Rourke
 25 T.D. et al., 1998), mainly due to the absence of extensive instrumental records of the seismic
 26 ground motion. The measure is defined according to an index scale, with each level having a
 27 qualitative description of earthquake effects on constructions and natural surroundings, as well
 28 as on human perceptions. The subjective nature of its definition, introduces a high level on
 29 uncertainty, making *MMI* an inadequate *IM* for a quantitative seismic risk assessment of
 30 pipelines.

4.2.2 Peak Ground Acceleration (PGA)

PGA constitutes the most common measure of the amplitude of a seismic ground motion and it was widely used as seismic *IM* for above ground structures, such as buildings and bridges. This seismic *IM* can easily be obtained from recorded accelerograms, as follows:

$$PGA = \max |a(t)| \quad (7)$$

In the absence of recorded data, use of Ground Motion Prediction Equations (GMPE) or shake maps that are made available few minutes after a seismic event, can be made. Alternatively, stochastic simulation of ground motion may be applied, particularly during pre-seismic evaluations of existing networks.

PGA correlates directly with the inertial response of a structure, which in cases of buried pipelines is of minor, if not negligible, importance. However, PGA was extensively used as seismic *IM* in seismic fragility functions for pipelines, especially in early studies (Katayama et al., 1975; Isoyama and Katayama, 1982; TCLEE-ASCE, 1991; Hamada, 1991; O'Rourke T.D. et al., 1991, Isoyama et al., 2000; O'Rourke T.D. et al., 1998; Chen et al., 2002; Lee et al., 2016). Figure 6 compares PGA-based empirical fragility relations developed on the basis of damage reports of cast-iron buried pipelines. The comparison reveals significant deviations in the prediction of repair rates, even for the area of common range of applicability of the relations, as reported by Tromans (2004) and highlighted with purple box in figure. Obviously, the observed deviations may be attributed to the range and quality of the dataset of damage reports and the regression analysis used to develop each relation, as well as to issues related to the rational evaluation of PGA, particularly in cases of earlier studies, where relevant recorded data and reliable GMPE were absent. However, the high differences of the relations could be an evidence of the poor 'efficiency' of PGA to correlate with observed damages on pipelines.

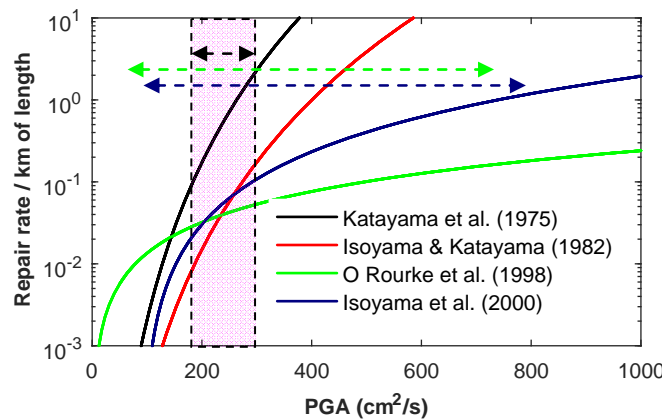


Figure 6. Comparison of PGA-based empirical fragility relations for cast iron pipelines. Dashed lines highlight the applicability range of the relations (adapted after Tromans, 2004).

Various definitions of PGA may be found in the relevant literature, referring to above ground structures, including the use of (i) the peak value of the two orthogonal directions at a given location, (ii) the average of the peak values of the orthogonal directions, (iii) the square root of

1 the sum of squares (SRSS) of the two orthogonal directions, (iv) the maximum amplitude of
2 the resultant (RES) vector of the orthogonal directions and (v) the geometric mean of the
3 orthogonal directions. The most ‘adequate’ value for the evaluation of the seismic vulnerability
4 of pipelines is generally an open issue, calling for further investigation.

6 **4.2.3 Peak Ground Velocity (PGV)**

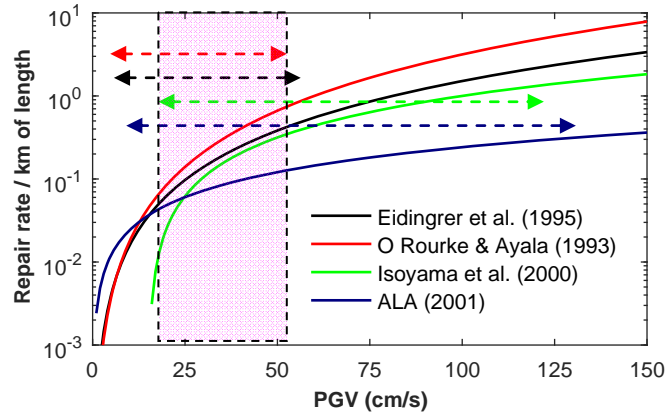
7 *PGV* was used extensively as seismic *IM* in fragility relations for buried pipelines (Barenberg,
8 1988; O’Rourke M.J. and Ayala, 1993; Eidinger et al., 1995; Eidinger et al., 1998; Jeon and
9 O’Rourke T.D., 1995; O’Rourke et al., 1998; Isoyama et al., 2000; ALA, 2001; Chen et al.,
10 2002; Pineda and Ordaz, 2003; O’Rourke M.J. and Deyoe, 2004; Lanzano et al., 2013;
11 Lanzano et al., 2014; Jahangiri and Shakib, 2018). The wide use of *PGV* is attributed to its
12 direct relation with the longitudinal ground strain, which is responsible for the induced
13 damages on buried pipelines caused by transient ground deformations. The relation between
14 *PGV* and ground strain is further examined in the following section. Velocity time histories
15 may be obtained through integration of accelerograms recorded at the site of interest.
16 Subsequently, *PGV* can be obtained as follows:

$$17 \quad PGV = \max |v(t)| \quad (8)$$

18 In the absence of acceleration time history recordings, *PGV* may be obtained either through
19 GMPEs that correlate directly *PGV* with multiple seismological parameters, or by the use of
20 relevant shake maps. Additionally, *PGV/PGA* relations have also been proposed in relevant
21 guidelines and research papers (e.g. ALA, 2001; Hashash et al., 2001), which may be used in
22 the absence of more rigorous *PGV* data. However, the efficiency of the latter is rather reduced,
23 particularly for soft soils, where the seismic vulnerability of pipelines is generally amplified
24 (ALA, 2001; Jahangiri and Shakib, 2018).

25 Figure 7 compares the *PGV*-based fragility relations, which according to Gehl et al. (2014) are
26 considered to be more adequate in describing the vulnerability of continuous NG pipelines.
27 Noticeable deviations between the fragility relations are observed again, even for the common
28 range of applicability (highlighted with the purple box in figure). However, these deviations
29 are lower compared to those observed in the relevant comparisons of *PGA*-based relations
30 (Figure 6), highlighting a better ‘performance’ of this metric against *PGA*. This observation
31 comes in line with several studies, which highlighted the superiority of *PGV* as seismic *IM* for
32 buried pipelines compared to *PGA*. For instance, *PGV* was reported as more efficient seismic
33 *IM* for describing the observed damages of water-supply buried pipelines in the comparative
34 study of Jeon and O’Rourke T.D. (2005). Using damage reports of the medium- and low
35 pressure NG network of L’Aquila, Italy, during the 2009 earthquake, Esposito et al. (2014)
36 estimated repair rates, which were plotted against local-scale *PGV* values. The latter was
37 defined using shake maps that illustrated the spatial distribution of *PGV* in the region. The
38 above correlations indicated a higher concentration of damages in areas with higher reported

1 *PGV*. However, the comparisons of the estimated repair rates with the predictions of
 2 commonly used *PGV*-based fragility functions, i.e. NIBS (2004), Eidinger et al. (1998) and
 3 ALA (2001), revealed a general under prediction of the expected damage by the latter. The
 4 observed differences were associated to the differences of the structural characteristics of the
 5 L'Aquila NG network, compared to the characteristics of the networks, for which the fragility
 6 relations were developed. A reasonably good coloration between observed damages on buried
 7 pipelines and *PGV* was also reported in the case of the water-supply network of the city of
 8 Darfield during the 2011 earthquake sequence in New Zealand (O'Rourke T.D. et al., 2014).
 9 The repair/damage spots were generally concentrated in the areas, where a higher *PGV* was
 10 reported. It is worth noticing the different definition of *PGV* in the studies of Esposito et al.
 11 (2014) and O'Rourke T.D. et al. (2014). In the former study, *PGV* was defined as the peak
 12 value of one of the orthogonal directions. On the contrary, the geometric mean of *PGV* of the
 13 two orthogonal directions was used in the latter study. These different computational
 14 approaches highlight again the open issue of the 'proper' way of evaluating instrumental
 15 seismic *IMs*. Similar to *PGA*, *PGV* can be defined in various ways, e.g. peak value, SRSS
 16 value, RES value etc. In a relevant study, Jeon and O'Rourke T.D. (2005) reported a higher
 17 level of correlation between damages/repairs of cast iron buried pipes during the 1994
 18 Northridge earthquake and *PGV* values, the latter computed on the basis of peak values of one
 19 of the orthogonal directions.



20
 21 **Figure 7.** Comparison of *PGV*-based empirical fragility relations for buried pipelines (ALA relation
 22 refers to the backbone curve, i.e. $K_I=1.0$). Dashed lines highlight the applicability range of the relations
 23 (adapted after Tromans, 2004).
 24

25 4.2.4 Peak ground strain (ϵ_g)

26 The longitudinal ground strain constitutes the main loading mechanism of buried pipelines
 27 subjected to seismically-induced transient ground deformations; therefore, it is directly related
 28 to the seismic performance and vulnerability of this infrastructure. In this context, the peak
 29 ground strain ϵ_g was used as seismic *IM* for buried pipelines in some recent studies (O'Rourke
 30 M.J. and Deyoe, 2004; O'Rourke M.J., 2009; O'Rourke T.D. et al., 2014; O'Rourke M.J.,

2015). ε_g may be quantified rigorously from ground displacement time histories along the axis of the pipeline, as follows (Pineda-Porras and Najafi, 2008):

$$\varepsilon_g = \max |\varepsilon(t)| = \max |\partial D(t)/\partial t| \quad (9)$$

The required displacement time histories may be evaluated via double integration of accelerographs at the site of interest. Considering the inaccuracies in the processing of the raw acceleration data, including the potential effects of filtering and base line correction or tapering, the accuracy of the computed displacement time histories might be debatable. More importantly, the above procedure requires a number of records along the pipeline axis, which should be referenced to an absolute time reference (Pineda-Porras and Najafi, 2008). Therefore, the installation of dense seismic arrays along the pipeline axis is necessary. However, the high installation and operation costs of such arrays impede such a selection in extended NG networks. Along these lines, it is common in practice to evaluate ε_g in a simplified fashion, using the *PGV*, as follows:

$$\varepsilon_g = PGV/\kappa C \quad (10)$$

where C is a measure of the wave propagation velocity and κ is a correction parameter to account for the maximization of strain as a function of the incidence angle φ , the latter formed between the plane wave propagation and the longitudinal axis of the pipeline. The selection of C and κ depends on the wave type, the incidence angle and the local soil conditions. In this context, the dominant seismic wave type at the area of interest should be initially defined. Generally, body waves and particularly shear *S*-waves, are expected to dominate the response of a pipeline located near the seismic source, while for pipelines located away from the seismic source, surface Rayleigh waves are manifesting the response. IITK-GSDMA (2007) guidelines suggested a limit for the selection of the ‘appropriate’ seismic waves for design purposes, which may potentially be used for vulnerability assessment purposes, as well. In particular, *S*-waves should be used for the design or assessment of pipelines located at an epicentral distance up to five times the focal depth, whereas for higher distances, *R*-waves should be considered. The apparent velocity C in Equation 10 may be defined on the basis of above recommendations for the dominant seismic waves.

Quite distinct recommendations may be found in relevant guidelines for the determination of the above parameters in case of *S*-waves. ALA (2001) suggests the use of $C = 2$ km/s, and $\kappa = 2.0$ for *S*-waves. The AFPS/AFTES (2001) guidelines for the seismic design of tunnels suggests $\kappa = 2.0$ and C to be taken as the minimum value between 1 km/s and a mean soil shear wave velocity of the upper subsurface, the latter corresponding to a depth equal to the fundamental wavelength of soil deposit. Eurocode 8 (EN1998-4, CEN 2006) proposes the ‘apparent wave speed’ C to be computed based on geophysical considerations, while implicitly κ is set equal to 1.0. Significant differences may be found on the selection of the apparent velocity of relevant studies that proposed ε_g -based fragility functions for buried pipelines, as well. O’Rourke M.J. and Deyoe (2004) adopted in their study apparent velocities C equal to

1 500 m/s and 3000 m/s for *R-waves* and *S-waves*, respectively. Following Paolucci and
2 Smerzini (2008), O'Rourke M.J. (2009) used an apparent velocity $C = 1000$ m/s to update his
3 previous fragility function (O'Rourke M.J. and Deyoe, 2004). Comparing the above
4 recommendations and studies, one can get twice as high ground strains, when implementing
5 the ALA guidelines compared to AFPS/AFTES, while the empirical fragility relations
6 proposed for *S-waves* by O'Rourke M.J. and Deyoe (2004) and O'Rourke M.J. (2009) on the
7 basis of similar damage reports may provide highly distinct predictions for the expected
8 damage of a network.

9 For surface *R-waves*, κ is equal to 1.0, while C is equal to phase velocity, c_{ph} (O'Rourke M.J.
10 and Liu, 1999). The phase velocity is defined as the velocity at which a transient vertical
11 disturbance of a given frequency that originates at ground surface is propagating across the
12 surface of the soil site. This velocity is related to wavelength λ and frequency f of the
13 disturbance, as follows: $c_{ph} = \lambda f$. Dispersion curves have been proposed in the literature to
14 account for this frequency dependence of c_{ph} in case of layered soil profiles, resting on elastic
15 half space (O'Rourke M.J. and Liu, 1999). O'Rourke M.J. et al. (1984) highlighted that for low
16 frequencies, the effect of the characteristics of the soil deposits, overlaying the half space, on
17 the c_{ph} is negligible since the corresponding wavelength is larger than the thickness of the
18 overlying soil layer. Hence, c_{ph} is slightly lower than the shear wave velocity of the elastic half
19 space. For high frequencies, the wavelength is comparable to the thickness of the overlying soil
20 layer and therefore the phase velocity is affected highly by its characteristics. A tri-linear
21 relation between the phase velocity and the frequency was proposed by O'Rourke M.J. et al.
22 (1984) on the basis of the above observations. The correlation of the phase velocity with the
23 wavelength highlights the importance of an 'adequate selection' of the later in the definition of
24 the ground strain. Some suggestions on the selection of this critical parameter may be found in
25 the literature (O'Rourke M.J. et al., 1984). However, its accurate determination is still an open
26 issue.

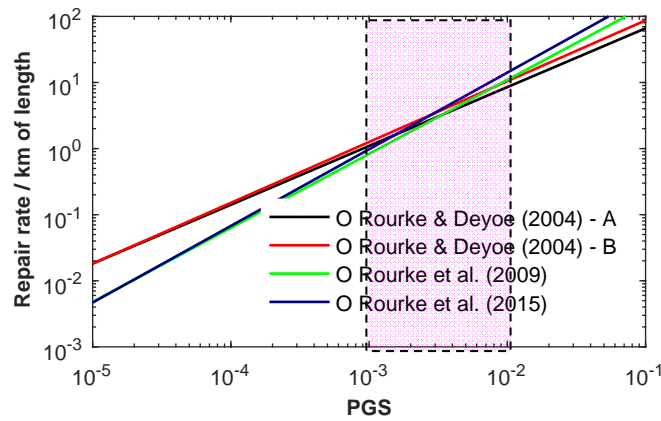
27 The above discussion and observations highlight the uncertainty introduced in the evaluation of
28 ε_g , even for the cases of relatively homogeneous soil deposits. The evaluation of ε_g becomes
29 more complex in cases of irregular topography (e.g. variable bedrock depth, hills, canyons,
30 slopes), as well as in the presence of significant lateral soil heterogeneities. Actually, in such
31 conditions the seismic vulnerability of pipelines is expected to increase significantly (e.g.
32 Trifunac and Todorovska, 1997; Takada et al., 2002; Scandella and Paolucci, 2006; Psyrras
33 and Sextos, 2018), while a worse correlation between the ε_g and PGV is commonly observed
34 (Paolucci and Pitilakis, 2007). Several approaches have been proposed in the literature to
35 account for the effects of irregular topography on the ground strain in a simplified fashion.
36 Indicatively, O'Rourke M.J. and Liu (1999) presented a simplified procedure for the
37 computation of the ground strain in cases of soil deposits with inclined soil-bedrock interface,
38 while Scandella and Paolucci (2006) proposed an analytical relationship for the ε_g - PGV

1 correlation near the boundaries of basins with simplified geometries. Numerous studies that
2 examine the effects of topography and soil heterogeneous soil condition on the soil straining
3 response may be found in the literature. A detailed presentation of this aspect is out of the
4 scope of this paper.

5 The implementation of ε_g -based fragility relations requires the development of seismic hazard
6 maps in terms of ε_g . The latter can be obtained either by converting *PGV* shake maps,
7 implementing Equation 10 and making ‘adequate’ selections for the apparent velocity *C*.
8 Alternatively, ε_g hazard maps can be computed on the basis of 2D or even 3D soil response
9 analyses for seismic ground motions compatible with the targeted seismic hazard. The
10 implementation of numerical simulations, especially in 2D or 3D, requires a significant
11 computational effort and time; hence, this approach is not efficient for a rapid post-earthquake
12 assessment of extended pipeline networks. However, it may be used for networks of great
13 importance during pre-seismic vulnerability studies. In an alternative approach, a large number
14 of 1D soil response analyses may be employed to estimate the spatial distribution of seismic
15 hazard at the site of interest (Paolucci and Pitilakis, 2007). The 1D soil response analyses have
16 the advantage of computational efficiency, compared to 2D or 3D numerical analyses. The
17 main drawback is that 1D response analyses provide the soil strains that are of pure shear
18 nature (vertically propagated *S-waves* are used as input for these analyses). These strains
19 commonly have a relatively sharp variation with depth and more importantly, they cannot be
20 translated into longitudinal soil strain in a straightforward way. Another drawback of 1D soil
21 response analyses is that these analyses neglect the effects of lateral variation of the soil
22 properties, as well as the creation and propagation of surface waves, which may be important
23 for the response of pipelines, especially those located away from the epicenter of the seismic
24 event. Comparing numerically predicted shear and longitudinal soil strains, computed in
25 various depths by 1D and 2D soil response analyses, respectively, Paolucci and Pitilakis (2007)
26 reported a rather weak correlation between the two strains, which was generally increased with
27 increasing burial depth. Despite the above observations, the researchers suggested the use of
28 shear strains as a first approximation of the ground strains for the assessment of buried
29 pipelines, mainly due to the computational efficiency of 1D soil response analyses compared to
30 the other types of soil response numerical analyses. Regardless of the selected soil response
31 analysis method, the use of fully coherent ground seismic motions may lead to a significant
32 underestimation of the actual ground strains that may be developed along the axis of an
33 extended pipeline. Among others, Zerva (1993) highlighted the significant effect of variability
34 of shape of motions over the pipeline length on the induced strains on it.

35 Figure 8 compares ε_g -based fragility relations proposed for buried pipelines subjected to
36 seismically-induced transient ground deformations. The relations are plotted on the log-log
37 space. As reported by Psyrras and Sextos (2018), the relations provide comparable repair rates
38 for strain levels, ranging between 10^{-3} and 10^{-2} , which are highlighted with the purple box in
39 the figure. These strain levels are considered quite high to induce significant damages on

1 buried NG pipelines. For strain levels other than these, significant deviations between the
 2 relations are observed. However, these differences are generally lower compared to the
 3 relevant deviations observed in cases of *PGA*- and *PGV*- based fragility relations. It is worth
 4 noticing the increasing trend of damage rate with increasing ground strain level that is revealed
 5 by the fragility relations. As pointed out by Psyrras and Sextos (2018), this observation comes
 6 in contrast with early analytical studies (O'Rourke M.J. and Hmadi, 1988). The latter suggest
 7 that slippage phenomena between the pipeline and the surrounding ground are expected take
 8 place, even with the mobilization of small relative displacement, subsequently reducing the
 9 straining induced on the pipeline. The slippage phenomena and their effect on the pipe
 10 response are expected to be amplified with increasing ground strain level. Along these lines,
 11 the proposed functional form that is used to develop the fragility functions needs to be re-
 12 evaluated.



13
 14 **Figure 8.** Comparison of ε_g -based empirical fragility relations for buried pipelines subjected transient ground
 15 deformations (adapted after Psyrras and Sextos, 2018).

16
 17 The installation of distributed fiber optic sensing, capable of recording the strain level of the
 18 pipeline along its axis (e.g. Gastineau et al., 2009), in conjunction with the use of ε_g -based
 19 fragility relations may contribute towards a rapid post-earthquake assessment of extended
 20 pipeline networks, providing an almost real-time evaluation of the pipe straining and detection
 21 of damages. Since the ground strains are used in the definition of the ε_g -based fragility
 22 relations, this assessment framework might be more effective for the cases, where the pipe
 23 shares the same strain level with surrounding ground. As highlighted above, this condition is
 24 rarely valid, since slippage phenomena of the pipeline relative to the surrounding ground may
 25 take place even for low shaking motions (O'Rourke M.J. and Hmadi, 1988). Another drawback
 26 of the implementation of distributed fiber optic sensing is the high costs of installation and
 27 operation of these monitoring systems.

28
 29 **4.2.5 PGV^2/PGA**

30 *PGV*²/*PGA* was proposed by Pineda-Porras and Ordaz (2007) as a seismic *IM* for assessment
 31 of shallow pipelines embedded in soft soils. Dimensionally, this metric corresponds to

1 displacement and when modified by a relevant correction factor (the so-called shape factor λ_{pr})
 2 is shown to be an effective proxy for peak ground displacement (PGD). The latter is related
 3 with the very-low frequency content of seismic ground motion, which subsequently is
 4 associated with higher imposed ground deformations and strains on the pipeline. Along these
 5 lines, PGV^2/PGA might be a suitable candidate as seismic IM for buried pipelines. This IM
 6 may be estimated through shake maps or by making use of GMPEs for PGA and PGV , as
 7 shown in the previous sections. Pineda-Porras and Ordaz (2007) examined the performance of
 8 this seismic IM using reported repairs/damages of the water-supply system of Mexico City
 9 during the 1985 Michoacán earthquake. The study revealed a better correlation between the
 10 repairs/damages and PGV^2/PGA was reported, compared to PGV alone. However, this
 11 constitutes the only case where this seismic IM was used and validated. Given the peculiarities
 12 of the specific site and seismic event, further validation of the particular seismic IM is deemed
 13 necessary.

14
 15 **4.2.6 Arias Intensity (I_a)**

16 The seismic fragility of pipelines may be affected by the duration of strong seismic motion.
 17 Under certain circumstances, repeated ground strains of moderate amplitude, imposed over an
 18 extended period on the pipeline, may lead to higher levels of damage compared to
 19 instantaneous higher amplitude ground strains. Actually, a number of moderate loading cycles
 20 may cause cumulative cyclic damage on the pipeline, such as buckling phenomena on steel
 21 pipelines or fatigue on HDPE pipelines. In this context, Arias intensity I_a , may be considered
 22 as a potential seismic IM for the characterization of the structural performance of buried steel
 23 NG pipelines since it embodies both the amplitude and duration characteristics of the seismic
 24 ground motion. Arias intensity I_a , may be defined as follows:

25
$$I_a = \frac{\pi}{2g_0} \int_0^{\infty} [a(t)]^2 dt \quad (11)$$

26 where $a(t)$ is an acceleration time history. Among other seismic IMs , O'Rourke et al. (1998)
 27 examined the 'efficiency' (in a general sense) of I_a for buried pipelines, reporting a poor
 28 correlation between this seismic IM and observed damages. Contrarily, Hwang et al. (2004)
 29 reported a higher level of correlation between I_a and reported damages on the NG network of
 30 Taichung City during the 1999 Chi-Chi earthquake, compared to other seismic IMs , such as
 31 PGA , PGV and spectral intensity SI . However, the latter study was based on limited data from
 32 one case study. A potential drawback of I_a is the large number of recorded acceleration time
 33 histories that are required to obtain the spatial variability of this metric along the length of the
 34 pipeline axis. Therefore, the use of a dense instrumentation array is mandatory; however, the
 35 high installation and operation costs of such an array may impede the extended use of this
 36 seismic IM .

37

4.2.7 Spectral Acceleration (S_a) and Spectrum Intensity (SI)

The spectral acceleration S_a constitutes a meter of the ‘strength’ of the seismic ground motion that may adversely affect structures at given frequencies. It actually describes the seismic motion as a function of the response of elastic single degree of freedom oscillators (SDOF) with ξ % damping and natural periods T . S_a was widely used as seismic IM for above ground structures, such as building and bridges, since it is related directly with the inertial response of the structure, which is controlling the seismic response of the structure itself.

The spectrum intensity, on the other hand, is computed as:

$$SI(\xi) = \frac{1}{C_1} \int_{t_1}^{t_2} S_v(\xi, T) dT \quad (12)$$

where T is the natural period of the structure, S_v is the velocity response spectrum, ξ is the damping of the structure and C_1 , t_1 and t_2 are constants. In the original formulation proposed by Housner (1952), C_1 , t_1 and t_2 were set equal to 1, 0.1 s and 2.5 s, respectively, while other definitions for the above parameters may be found in the literature. Similar to Arias Intensity, a series of records of the seismic ground motion (e.g. acceleration time histories) is required along the pipeline axis, to estimate the spatial distribution of both the spectral acceleration S_a and spectrum intensity SI . With reference to the applicability of the above seismic IM in cases of buried pipelines, O’Rourke et al. (1998) investigated the efficiency (in the general sense) of SA to correlate with observed damages on buried cast iron pipelines of the water-supply system of California during the 1994 Northridge earthquake. In a similar study, Hwang et al. (2004) examined the use of SI for embedded pipelines, by implementing damage reports on gas and water-supply pipelines of Taichung City during the 1999 Chi-Chi earthquake. In both studies, the above seismic IMs were found to provide very poor correlations with the reported damages. These poor correlations are actually expected, since both IM are directly related to the inertial response of above ground elastic single degree of freedom oscillators, the seismic response of which is highly distinct compared to the one that the embedded pipelines exhibit.

4.2.8 Peak ground shear strain (γ_{max})

Trifunac and Todorovska (1997) established fragility relations using damage reports of buried pipelines in California during the 1994 Northridge earthquake. In their study the peak ground shear strain γ_{max} was used as seismic IM . Despite the differences between the shear and axial ground strains (see Section 4.2.3), the evaluation of the spatial distribution of peak ground shear strain in a site of relatively known properties is by far an easier task compared to the evaluation of the axial soil strains. In their study, Trifunac and Todorovska (1997) used the following simplified formula to define approximately the peak soil shear strain:

$$\gamma_{max} = \frac{PGV}{V_{s,30}} \quad (13)$$

1 where $V_{s,30}$ is the average shear wave velocity of the top 30 m of soil deposits. Obviously, such
2 a definition requires the knowledge of the spatial distribution of PGV , as well as $V_{s,30}$. As stated
3 above, the former may be defined by making use of shake maps that are published after a
4 particular seismic event, or via GMPEs. $V_{s,30}$ may be obtained using available geological and
5 geotechnical data for the given site. For pre-seismic assessments of existing NG networks, an
6 extended use of 1D soil response analyses, covering the area of interest and accounting for the
7 geological, geomorphic and geotechnical data of the site, could provide a better idea of the
8 spatial distribution of γ_{max} .

10 **4.3 On the efficiency and sufficiency of seismic IM for buried steel NG pipelines**

11 Employing a numerical framework, Shakid and Jahangiri (2016) examined the efficiency and
12 sufficiency of 18 seismic IMs for buried steel NG pipelines, in a mathematically rigorous way
13 (Baker and Cornell, 2005, Luco and Cornell, 2007). The investigated seismic IM are
14 summarized in Table 4. Their analysis included IDA of six small-diameter API 5L X65 steel
15 NG pipelines embedded in soft to medium-stiff uniform soil deposits. In particular, the selected
16 pipe diameters were ranged between 356 mm and 610 mm, while the selected diameter over
17 thickness ratios (D/t) varied between 45.1 and 95.3. The internal pressure of the pipelines was
18 ranged between 1.7 MPa and 5.2 MPa, while the burial over diameter ratios (H/D) varied
19 between 2.5 and 5.4. Finally, the shear wave propagation velocity of the surrounding ground
20 was ranging between 180 m/s and 360 m/s. A finite length of the selected pipelines was
21 modelled by means of inelastic shell elements, whilst the effect of infinite length of the
22 pipeline on the actual response was considered by means of nonlinear axial springs, which
23 were introduced at both end-sides of the pipeline, following Liu et al. (2014). The surrounding
24 ground was modelled by nonlinear spring elements, acting in the axial, transverse and vertical
25 directions, defined as per ALA (2001) guidelines, while dashpots elements were also
26 introduced, following Hindy and Novak (1979). The IDA was conducted using an assembly of
27 30 real far-field seismic ground motions, scaled to various PGA in steps of 0.1 g. The
28 computed by the dynamic analyses peak axial compression strain of the pipeline was used as
29 EPD . The effects of spatial distribution and incoherence of the seismic ground motion, as well
30 as potential soil heterogeneities along the pipelines axis were not considered. In addition to the
31 previously discussed seismic IMs (e.g. PGA , PGV , PGV^2/PGA , I_a), a set of new seismic IMs
32 was also examined. A brief presentation of these new seismic IMs is made in the ensuing,
33 examining their potential application in buried pipelines, while the main conclusions of this
34 study are finally discussed.

1 **Table 4.** Seismic IM investigated by Shakib and Jahangiri (2016)

#	Seismic IM	#	Seismic IM
1	Peak ground acceleration, PGA	10	Cumulative absolute velocity, CAV
2	Peak ground velocity, PGV	11	Acceleration spectrum intensity, ASI
3	Peak ground displacement, PGD	12	Velocity spectrum intensity, VSI
4	PGV^2/PGA	13	Sustained maximum acceleration, SMA
5	Root mean square acceleration, RMS_a	14	Sustained maximum velocity, SMV
6	Root mean square velocity, RMS_v	15	Spectral acceleration, $S_a(T_1, 5\%)$
7	Root mean square displacement, RMS_d	16	Spectral velocity, $S_v(T_1, 5\%)$
8	Arias Intensity, I_a	17	Spectral displacement, $S_d(T_1, 5\%)$
9	PGD^2/PMS_d	18	$\sqrt{VSI \times [\omega_1 \times (PGD + RMS_d)]}$

2

3 **4.3.1 Peak Ground Displacement, PGD**

4 PGD corresponds to the maximum absolute value of a ground displacement time history, i.e.:

$$5 \quad PGD = \max |d(t)| \quad (14)$$

6 The required for the computation of PGD , ground displacement time histories are commonly
7 defined through double integration of acceleration time histories recorded at the site of interest.
8 As stated already, PGD correlates better with the longer period ordinates of ground seismic
9 motion, which generally are associated with higher ground deformations and higher straining
10 on buried pipelines. Along these lines, PGD may be considered as an adequate candidate of a
11 seismic IM for buried NG pipelines. However, the inherent uncertainties associated with the
12 integration analysis of acceleration time histories are unavoidably propagate in the computation
13 of this seismic IM .

14

15 **4.3.2 Root mean square acceleration, RMS_a , velocity, RMS_v , and displacement, RMS_d**

16 The root mean square acceleration is determined using acceleration recordings at a site, as
17 follows:

$$18 \quad RMS_a = \sqrt{\frac{1}{t_e - t_0} \int_{t_0}^{t_e} [a(t)]^2 dt} \quad (15)$$

19 where t_0 and t_e indicate the beginning and end of the duration of the seismic ground motion
20 under consideration. This seismic IM constitutes a measure of the average rate of energy
21 imparted by the ground seismic motion. The large number of recorded acceleration time
22 histories that is required to obtain the spatial variability of RMS_a , impedes the wide use of this
23 seismic IM for extended networks of buried pipelines. Similar relations with Equation 15 may
24 be found in the literature for the definitions of the root mean square velocity RMS_v and the root
25 mean square displacement RMS_d , which are rarely used in practice.

26

27

28

4.3.3 Cumulative absolute velocity, CAV

The cumulative absolute velocity (CAV) has a similar interpretation to RMS_a , as it is actually derived by integrating the entire ground acceleration recording, as follows:

$$CAV = \int_0^t |a(t)| dt \quad (16)$$

The use of RMS_a or CAV as seismic IMs for buried pipelines might be questionable, since both measures are associated directly with the ground acceleration. As already discussed, ground acceleration is related to inertial loads, which are generally of secondary importance for the seismic response and vulnerability of buried civil infrastructure.

4.3.4 PGD^2/RMS_d

PGD^2/RMS_d constitutes a dimensionless metric of the ground displacement. The evaluation of this seismic IM requires the definition of the PGD and RMS_d , which both depend on the estimation of displacement time histories through the double integration of acceleration time histories recordings at the site of interest.

4.3.5 Sustained maximum acceleration, SMA , and velocity, SMV

The sustained maximum acceleration SMA and the sustained maximum velocity SMV , which both were defined by Nuttli (1979), characterize the seismic ground motion using lower peaks of the recorded acceleration or the velocity time histories. In particular, SMA is defined as the third (or fifth) highest (absolute) value of the acceleration time history, while SMV is defined in a similar manner using the velocity time history. Obviously, accelerographs from the investigated site are required for the definition of these seismic IMs .

4.3.6 Spectral seismic IMs

The acceleration response spectrum, S_a , is commonly calculated using the Nigam and Jennings (1969) algorithm. The spectral velocity, S_v , and spectral displacement, S_d , may then be estimated, based on the following relations (Chopra, 1995):

$$S_v(T) = \left(\frac{2\pi}{T}\right) \times S_d(T), \quad S_a(T) = \left(\frac{2\pi}{T}\right)^2 \times S_d(T) \quad (17)$$

Having estimated the response spectra for a given seismic ground motion time history, the acceleration and velocity spectra intensities, ASI , VSI , may be defined by integrating the relevant response spectra, as follows:

$$ASI = \int_{0.1}^{0.5} S_a(T) dT, \quad VSI = \int_{0.1}^{0.5} S_v(T) dT \quad (18)$$

In addition to the above spectral seismic IMs , Shakib and Jahangiri (2016) examined the efficiency and sufficiency of the following vector seismic IM : $\sqrt{VSI \times [\omega_1 \times (PGD + RMS_d)]}$,

1 where ω_1 is the first natural frequency of the pipe-soil configuration. According to the
2 researchers, ω_1 is quantified on the basis of a natural frequency analysis, using the numerical
3 models of the soil-pipeline configuration presented above (i.e. pipe shell model on soil
4 springs). In the authors' view, the use of spectral seismic *IMs*, as well as the definition of ω_1
5 for embedded structures, such as buried pipelines, are not straightforward tasks. More
6 importantly, the use of spectral seismic *IMs* seems to be not valid from a theoretical viewpoint,
7 especially when considering the prevailing loading mechanism of buried pipelines during
8 seismic ground shaking. As highlighted in several parts of the paper, the seismic response of
9 buried pipelines is dominated by the kinematic loading imposed by the surrounding ground on
10 them, while, contrary to above ground structures, their inertial response is of secondary, if not
11 negligible, importance. Additionally, the response of buried structures is highly distinct
12 compared to that of a single degree of freedom oscillator (SDOF), for which the response
13 spectra and the relevant spectral seismic *IMs* are actually defined. In this context, the use of
14 spectral seismic *IM* for embedded civil infrastructure, such as buried pipelines, is highly
15 arguable. These perspectives come in line with the poor correlations between spectral seismic
16 *IMs*, i.e. spectral acceleration and spectrum intensity, and reported damages on water-supply
17 and steel NG pipelines during past earthquakes (O'Rourke M.J. et al., 1998; Hwang et al.,
18 2004).

19

20 **4.3.7 Summary**

21 The study of Shakib and Jahangiri (2016) revealed different *optimum* seismic *IM* for pipelines
22 embedded in soft or medium-stiff soil deposits. More specifically, for buried pipelines in soft
23 soils, $\sqrt{VSI \times [\omega_1 \times (PGD + RMS_d)]}$ revealed the higher efficiency and sufficiency compared to
24 other seismic *IMs*, while the next more efficient and sufficient seismic *IM* was found to be
25 RMS_d . On the contrary, PGD^2/RMS_d was found to be the optimum seismic *IM* for buried
26 pipelines in medium-stiff soils. It is worth noticing that the above conclusions were drawn for
27 pipelines with diameters $D < 800$ mm, without covering large-diameter pipelines that are
28 commonly found in transmission NG networks (diameters up to 1400 – 1800 mm).
29 Additionally, the operational pressure, which may affect significantly the axial response of a
30 pressurized steel pipeline, was restricted to 5.2 MPa. The operational pressure of transmission
31 NG networks may exceed this value, reaching 8.0 to 8.5 MPa. More importantly, the study did
32 not examine any relations between particular damage modes (e.g. local buckling) and seismic
33 *IMs*, neither investigated the critical effects of soil heterogeneities and spatial variability of the
34 seismic ground motion along the pipeline axis. An interesting point is that the same researchers
35 proposed in a later study numerical fragility curves for NG steel pipelines (see *Section 3.3*),
36 using *PGV* as seismic *IM* (Jahangiri and Shakib, 2018).

37

4.4 Identified gaps and challenges

Summarizing, *MMI* is considered an outdated *IM*, which due to its subjective definition is not appropriate for a quantitative seismic assessment. Theoretically, ε_g may directly be related to seismic vulnerability of buried pipelines. However, its evaluation might be more cumbersome compared to *PGV*, due to difficulties and uncertainties in the definition of the apparent wave velocity *C*. *PGA* is related directly with inertial forces, which for buried pipelines are not important. PGV^2/PGA requires the definition of two parameters, while its efficiency has not been extensively validated. I_a provides information of both the duration and amplitude of a seismic ground motion; however, its definition in field might be difficult, as a large number of accelerograms is required to evaluate its spatial distribution at the site of interest. Peak ground shear strain (γ_{max}) is not related directly to peak ground axial strain that imposes damages on buried pipelines. However, in a ground response analysis framework, γ_{max} may be evaluated easier than ground axial strain, since 1D soil response analyses suffice for its computation. The additional seismic *IMs* used by Shakib and Jahangiri (2016), e.g. *PGD*, RMS_a , RMS_v , RMS_d , PGD^2/PMS_d , *CAV*, *SMA*, *SMV*, etc. have not been validated against real reported damages of buried pipelines. However, some of them, such as *PGD* might be considered as promising candidates. Finally, in the authors' opinion, the use of spectral seismic *IMs* for buried pipelines is highly debatable.

One of the main issues that prevent the definition of the optimum seismic *IM* for a quantitative seismic assessment of NG pipelines is the lack of evidence on the efficiency (in the general sense) of various seismic *IMs* to correlate with particular damage modes of pipelines. This knowledge shortfall highlights the need for numerical and experimental studies, which will allow for a thorough investigation of the level of correlation of various damage modes of NG steel pipelines with various seismic *IMs*. A summary of numerical approaches that may be used towards this direction are presented in the second part of the paper.

5. Conclusions

The paper summarized a critical review of available fragility relations for the vulnerability assessment of buried NG pipelines subjected seismically-induced transient ground deformations. Particular emphasis was placed on the efficiency of various seismic *IMs* to be evaluated or measured in the field and, more importantly, to correlate with observed structural damages of this critical infrastructure. The main conclusions and identified open issues are summarized in the following:

- Distinct damage modes may have different consequences on the structural integrity and serviceability of buried steel NG pipelines. Understanding the main response mechanisms behind the identified damage modes on the basis of rigorous experimental and numerical studies, may contribute towards a reliable definition and quantification of limit states for this infrastructure.

- 1 • The majority of available empirical fragility relations refer to segmented cast-iron and
2 asbestos cement pipelines, the seismic response of which is quite distinct compared to
3 continuous pipelines, such as buried steel NG pipelines. Additionally, the implementation
4 of repair rate as an *EDP* does not provide any information regarding the severity of
5 damage, as well as the type of required repair. The most important drawback of empirical
6 fragility relations is that they do not disaggregate between the potential damage modes.
- 7 • The recently-developed analytical fragility functions for buried steel NG pipelines refer to a
8 limited number of soil-pipe configurations, while they do not consider many critical
9 parameters that may affect significantly the seismic response and vulnerability of this
10 infrastructure. Along these lines, additional research is deemed necessary towards the
11 development of analytical fragility functions, which will refer to distinct damage modes.
- 12 • Critical for development of efficient analytical fragility curves is the identification of
13 optimum seismic *IMs* for buried steel NG pipelines. The strengths and weaknesses of a
14 large number of commonly used seismic *IMs* for buried pipelines were discussed herein,
15 including also other potential metrics of the seismic intensity that may be found in the
16 literature. *PGV*, *PGD*, ε_g and PGV^2/PGA seem to be reasonable candidates as *optimum*
17 seismic *IMs* for structural assessment of buried NG pipelines, due to their compatibility
18 with the loading mechanism of buried pipelines under seismically-induced transient ground
19 deformations. On the contrary, the use of ‘spectral’ seismic *IMs* seems to be incompatible
20 with the loading mechanism and general behaviour of buried civil infrastructure. One of the
21 main issues that prevent the definition of optimum seismic *IMs* for buried steel NG
22 pipelines, to date, is the lack of evidence regarding the ‘efficiency’ of various seismic *IMs*
23 to correlate with particular damage modes of buried pipelines. This knowledge shortfall
24 highlights the need for efficient numerical methodologies, which will allow for a proper
25 simulation of the distinct damage modes of buried steel NG pipelines and a thorough
26 investigation of the level of correlation of these damage modes with various seismic *IMs*.

27 Alternative methods for the analytical evaluation of the vulnerability of buried steel NG
28 pipelines under seismically-induced transient ground deformations are thoroughly discussed in
29 the second part of this paper. The discussion focuses on the assessment against seismically-
30 induced buckling failures since these constitute critical damage modes for the structural
31 integrity of this infrastructure.

32 33 **Acknowledgements**

34 This work was supported by the Horizon 2020 Programme of the European Commission under
35 the MSCA-RISE-2015-691213-EXCHANGE-Risk grand (Experimental and Computational
36 Hybrid Assessment of NG Pipelines Exposed to Seismic Hazard, www.exchange-risk.eu). This
37 support is gratefully acknowledged.

1 **References**

- 2 AFPS/AFTES, 2001. Guidelines on earthquake design and protection of underground structures.
3 Working group of the French Association for Seismic Engineering (AFPS) and French Tunnelling
4 Association (AFTES), Version 1, Paris, France.
- 5 Ahmed, A.U., Aydin, M., Cheng, J.R., Zhou, J., 2011. (2011) Fracture of wrinkled pipes subjected to
6 monotonic deformation: An experimental investigation. *Journal of Pressure Vessel Technology*.
7 133, 011401.
- 8 ALA (American Lifelines Alliance), 2001. Seismic guidelines for water pipelines. Part 1- Guidelines.
9 ASCE-FEMA, Washington, DC, USA.
- 10 Alexoudi, M., 2005. Contribution to lifeline vulnerability in urban environment. Development of a
11 holistic methodology for seismic risk management. Phd Thesis, Aristotle University of
12 Thessaloniki, Thessaloniki, Greece.
- 13 American Lifelines Alliance. 2001a. Seismic Fragility Formulations for Water Systems. Part 1-
14 Guideline. ASCE-FEMA, 104 pp.
- 15 American Lifelines Alliance., 2001b. Seismic Fragility Formulations for Water Systems. Part 2 -
16 Appendices. ASCE-FEMA, 239 pp.
- 17 ASCE/TCLEE, 1991. Seismic loss estimation for a hypothetical water system. ASCE/TCLEE
18 Monograph No.2, C.E. Taylor (ed.).
- 19 Bai, Y., 2001. Pipelines and risers. Elsevier, Amsterdam
- 20 Bai, Q., Bai, Y., 2014. Subsea pipeline design, analysis, and installation. Elsevier, Amsterdam
- 21 Baker, J.W., Cornell, C.A., 2005. A vector-valued ground motion intensity measure consisting of
22 spectral acceleration and epsilon. *Earthquake Engineering and Structural Dynamics*. 34, 1193-1217.
- 23 Bakalis, K., Vamvatsikos, D., 2018. Seismic fragility functions via nonlinear response history analysis.
24 *ASCE Journal of Structural Engineering*. 144(10):04018181.
- 25 Ballantyne, D.B., Berg, E., Kennedy, J., Reneau, R., Wu D., 1990. Earthquake loss estimation modeling
26 for the Seattle water systems: Report to US Geological Survey under Grant 14-08-0001-G1526.
27 Technical Report, Kennedy/Jenks/Chilton, Federal Way, Washington, USA.
- 28 Barenberg, M.E., 1988. Correlation of pipeline damage with ground motions. *Journal of Geotechnical*
29 *Engineering, ASCE*, 114(6), 706-711.
- 30 Brazier, L.G., 1927. On the flexure of thin cylindrical shells and other 'thin' sections. *Proceedings of*
31 *the Royal Society, London, Series A*. 116, 104-114.
- 32 Chen, C.C., Ariman, T., Lee, L.N.H., 1980. Buckling analysis of buried pipelines under seismic loads.
33 *Proceedings of the 7th European Conference of Earthquake Engineering, 1980*, 249-256.
- 34 Chen, W., Shih, B.-J., Chen, Y.-C., Hung, J.-H., Hwang, H., 2002. Seismic response of natural gas and
35 water pipelines in the Ji-Ji earthquake. *Soil Dynamics and Earthquake Engineering*. 22, 1209-1214.
- 36 Chopra, A. K., 1995. *Dynamics of structures: Theory and application to earthquake engineering*.
37 Prentice Hall, New Jersey.
- 38 Cornell, C.A., and Krawinkler, H., 2000. Progress and challenges in seismic performance assessment.
39 *PEER Center News*. 32: 1 – 4.
- 40 De Risi, R., De Luca, F., Kwon, O.-S., Sextos, A., 2018. Scenario-based seismic risk assessment for
41 buried transmission gas pipelines at regional scale. *Journal of Pipeline Systems Engineering and*
42 *Practice*. 9(4).
- 43 Demirci, H.E., Bhattacharya, S., Karamitros, D., Alexander, N., 2018. Experimental and numerical
44 modelling of buried pipelines crossing reverse faults. *Soil Dynamics and Earthquake Engineering*.
45 114, 198-214.

1 Earthquake Engineering Research Institute, EERI, 1986. Reducing earthquake hazards: Lessons learned
2 from earthquakes. Earthquake Engineering Research Institute, El Cerrito, Publication n°86-02.

3 Eguchi, R.T., 1983. Seismic vulnerability models for underground pipes. Proceedings of Earthquake
4 Behavior and Safety of Oil and Gas Storage Facilities, Buried Pipelines and Equipment, PVP-77,
5 ASME, New York, 368-373.

6 Eguchi, R.T., 1991. Seismic hazard input for lifeline systems. Structural Safety. 10, 193-198.

7 Eiding J., 1998. Water distribution system. In: Anshel J. Schiff (ed.) The Loma Prieta, California,
8 Earthquake of October 17, 1989 – Lifelines. USGS Professional Paper 1552-A, US Government
9 Printing Office, Washington, A 63-A78.

10 Eiding, J., Maison, B., Lee, D., and Lau, B., 1995. East Bay municipal district water distribution
11 damage in 1989 Loma Prieta earthquake. Proceedings of the 4th US Conference on Lifeline
12 Earthquake Engineering, ASCE, TCLEE, Monograph 6, 240-24.

13 Elnashai, A.S., Di Sarno, L., 2015. Fundamentals of earthquake engineering. From source to fragility.
14 Wiley and Sons, UK.

15 Esposito, S., Giovinazzi, S., Elefante, L., Iervolino, I., 2013. Performance of the L'Aquila (central Italy)
16 gas distribution network in the 2009 (Mw 6.3) earthquake. Bulletin of Earthquake Engineering.
17 11(6), 2447-2466.

18 European Committee for Standardization (CEN), 2006. EN 1998-4: 2006. Eurocode 8: Design of
19 structures for earthquake resistance-Part 4: Silos, tanks and pipelines. European Committee for
20 Standardization, Brussels.

21 Fotopoulou, S., Ptilakis, K., 2015. Predictive relationships for seismically induced slope displacements
22 using numerical analysis results. Bulletin of Earthquake Engineering. 13(11), 3207-3238.

23 Gantes C.J., Bouckovalas G.D., 2013. Seismic verification of the high pressure natural gas pipeline
24 Komotini–Alexandroupoulis–Kipi in areas of active fault crossings. Structural Engineering
25 International.23(2),204-208.

26 Gastineau, A., Johnson, T., Schultz, A., 2009. Bridge health monitoring and inspections. A survey of
27 methods.

28 Gehl, P., Desramaut, N., Reveillere, A., Modaresi, H., 2014. Fragility functions of gas and oil
29 networks. SYNER-G: Typology definition and fragility functions for physical elements at seismic
30 risk, Geotechnical, Geological and Earthquake Engineering, Springer 27: 187-220.

31 Gresnigt, A.M., 1986. Plastic design of buried steel pipes in settlement areas. HERON. The
32 Netherlands, 31(4), 1-113.

33 Hamada, M., 1991. Estimation of earthquake damage to lifeline systems in Japan. Proceedings of the 3rd
34 Japan-US Workshop on Earthquake Resistant Design of Lifeline Facilities and Countermeasures for
35 Soil Liquefaction, San Francisco, CA, December 17-19, 1990. Technical Report NCEER-91-0001,
36 NCEER, State University of New York at Buffalo, Buffalo, NY, 5-22.

37 Hashash, Y.M.A., Hook, J.J., Schmidt, B., Yao, J.I.-C., 2001. Seismic design and analysis of
38 underground structures. Tunnelling and Underground and Space Technology. 16 (2), 247-293.

39 Hindy, A., Novak, M., 1979. Earthquake response of underground pipelines. Earthquake Engineering
40 and Structural Dynamics. 7, 451-476.

41 Honegger, D.G., Gailing, R.W., Nyman, D.J., 2002. Guidelines for the seismic design and assessment
42 of natural gas and liquid hydrocarbon pipelines. In the 4th International Pipeline Conference.
43 American Society of Mechanical Engineers, 563-570.

44 Honegger, D., Wijewickreme, D., Youd, T., 2014. Regional pipeline vulnerability assessment based
45 upon probabilistic lateral spread hazard characterization. In: Proceedings, 10th national conference
46 on earthquake engineering. EERI, Oakland.

1 Honegger, D.G., Wijewickreme, D., 2013. Seismic risk assessment for oil and gas pipelines.
2 Tesfamariam, S. and Goda, K. (eds.) Handbook of Seismic Risk Analysis and Management of Civil
3 Infrastructure Systems. Woodhead Publishing Series in Civil and Structural Engineering, 682-715.
4 Housner, G. W., 1952. Intensity of ground motion during strong earthquake. California Institute of
5 Technology. Pasadena, California.
6 Housner, G.W., Jennings, P.C., 1972. The San Fernando California earthquake. Earthquake
7 Engineering and Structural Dynamics. 1, 5-31.
8 Hwang, H., Chiu, Y.-H., Chen, W.Y., Shih, B.J., 2004. Analysis of damage to steel gas pipelines caused
9 by ground shaking effects during the Chi-Chi, Taiwan. Earthquake Spectra. 20(4), 1095-1110.
10 Hwang, H., Lin, H., 1997. GIS-based evaluation of seismic performance of water delivery systems.
11 Technical Report, CERl, the University of Memphis, Memphis.
12 IITK-GSDMA, 2007. Guidelines for seismic design of buried pipelines. Provisions with commentary
13 and explanatory examples. Indian Institute of Technology, Kanpur, India.
14 International Energy Agency, 2015. World energy outlook 2015. International Energy Agency, Paris,
15 France.
16 Isoyama, R., Katayama T., 1982. Reliability evaluation of water supply system during earthquakes.
17 Report of the Institute of Industrial science, University of Tokyo, 30 (1).
18 Isoyama, R., Ishida, E., Yune, K. and Shirozu, T., 2000. Seismic damage estimation procedure for water
19 supply pipelines. Proceedings of the 12th World Conference on Earthquake Engineering, Paper No.
20 1762.
21 Jahangiri, V., Shakib, H., 2018. Seismic risk assessment of buried steel gas pipelines under seismic
22 wave propagation based on fragility analysis. Bulletin of Earthquake Engineering. 16(3), 1571-1605.
23 Jalayer, F., Cornell, C.A., 2009. Alternative non-linear demand estimation methods for probability-
24 based seismic assessments. Earthquake Engineering and Structural Dynamics. 38(8), 951-972.
25 Jalayer, F., De Risi, R., Manfredi, G., 2015. Bayesian cloud analysis: efficient structural fragility
26 assessment using linear regression. Bulletin of Earthquake Engineering. 13(4), 1183-1203.
27 Jalayer, F., Ebrahimian, H., Miano, A., Manfredi, G., Sezen, H., 2017. Analytical fragility assessment
28 using unscaled ground motion records. Earthquake Engineering and Structural Dynamics. 46(15),
29 2639-2663.
30 Japan Gas Association, JGA, 2004. Seismic Design for Gas Pipelines, JG(G)-206-03, 91-100.
31 Jeon, S.S., O'Rourke, T.D., 2005. Northridge earthquake effects on pipelines and residential buildings.
32 Bulletin of Seismological Society of America. 95, 294-318.
33 Karamitros, D.K., Bouckovalas, G.D., Kouretzis, G.P., 2007. Stress analysis of buried steel pipelines at
34 strike-slip fault crossings. Soil Dynamics and Earthquake Engineering. 27, 200-211.
35 Karamitros, D., Zoupantis, C., Bouckovalas, G.D., 2016. Buried pipelines with bends: analytical
36 verification against permanent ground displacements. Canadian Geotechnical Journal. 53(11),
37 1782-1793.
38 Katayama, T, Kubo, K. and Sato, N., 1975. Earthquake damage to water and gas distribution systems.
39 Proceedings of the U.S. National Conference of Earthquake Engineering, Oakland, CA: EERI, 396-
40 405.
41 Kostinakis, K., Athanatopoulou, A., Morfidis, K., 2015. Correlation between ground motion intensity
42 measures and seismic damage of 3D R/C buildings. Engineering Structures. 82, 151-167.
43 Kouretzis, G., Krabbenhoft, K., Sheng, D., Sloan S.W., 2014. Soil-Buried pipeline interaction for
44 vertical downwards relative offset. Canadian Geotechnical Journal. 51, 1087-1094.

1 Kyriakides, S., Corona, E., 2007. Plastic buckling and collapse under axial compression. *Mechanical*
2 *Offshore Pipelines Buckling Collapse*, Vol. I, Elsevier Science, New York, 280-318.

3 Lanzano, G., Salzano, E., Santucci de Magistris, F., Fabbrocino, G., 2012. An observational analysis of
4 seismic vulnerability of industrial pipelines. *Chemical Engineering Transaction*. 26, 567-572.

5 Lanzano, G., Salzano, E., Santucci de Magistris, F., Fabbrocino, G., 2013. Seismic vulnerability of
6 natural gas pipelines. *Reliability Engineering and System Safety*. 117, 73-80.

7 Lanzano, G., Salzano, E., Santucci de Magistris, F., Fabbrocino, G., 2014. Seismic vulnerability of gas
8 and liquid buried pipelines, *Journal of Loss Prevention in the Process Industries*, 28, 72-78.

9 Lanzano, G., Santucci de Magistris, F., Fabbrocino, G., Salzano, E., 2015. Seismic damage to pipelines
10 in the framework of Na-Tech risk assessment. *Journal of Loss Prevention in the Process Industries*.
11 33, 159-172.

12 Lee, L.N.H., Ariman, T., Chen, C.C., 1984. Elastic-plastic buckling of buried pipelines by seismic
13 excitation. *International Journal of Soil Dynamics and Earthquake Engineering*. 3, 168-173.

14 Lee, D.H., Kim, B.H., Jeong, S.H., Jeon, J.S., Lee, T.H., 2016. Seismic fragility analysis of a buried gas
15 pipeline based on nonlinear time-history analysis. *International Journal of Steel Structures*. 16(1),
16 231-242.

17 Leville, T., Shane, D., Morris J., 1995. Northridge earthquake pipeline rupture into the Santa Clara
18 river. *Proceedings of the 1995 IOSC International Oil Spill Conference*, 489-494.

19 Liu, A., Hu, Y., Zhao, F., Li, X., Takada, S., Zhao, L., 2004, An equivalent-boundary method for the
20 shell analysis of buried pipelines under fault movement. *Acta Seismologica Sinica*. 17, 150-156.

21 Luco, N, and Cornell, C. A., 2007. Structure-specific scalar intensity measures for near-source and
22 ordinary earthquake ground motions. *Earthquake Spectra*, 232, 357-392.

23 Mackie, K., Stojadinovic, B., 2003. Seismic demands for performance-based design of bridges. In:
24 PEER Report 2003/16, University of California, Berkeley, CA.

25 McNorgan J.D., 1989. Relieving seismic stresses locked in gas pipelines. *Proceedings of the Second*
26 *U.S.-Japan Workshop on Liquefaction Large Ground Deformations and their Effects on Lifelines*.
27 *Technical Report NCEER-89-0032*, Multidisciplinary Center for Earthquake Engineering Research,
28 Buffalo, New York, 363-369.

29 Melissianos, V., Vamvatsikos, D., Gantes, C., 2017a. Performance-based assessment of protection
30 measures for buried pipes at strike-slip fault crossings. *Soil Dynamics and Earthquake Engineering*,
31 101, 1-11.

32 Melissianos, V., Lignos, X., Bachas, K.K., Gantes, C., 2017b. Experimental investigation of pipes with
33 flexible joints under fault rupture. *Journal of Constructional Steel Research*. 128,633-648.

34 Melissianos, V., Vamvatsikos, D., Gantes, C., 2017c. Performance assessment of buried pipelines at
35 fault crossings. *Earthquake Spectra*. 33(1), 201-218.

36 Meyersohn, W.D., O'Rourke, T.D., 1991. Pipeline buckling caused by compressive ground failure
37 during earthquakes. *Proceedings of the 3rd Japan-U.S. Workshop on Earthquake Resistance Design*
38 *of Lifeline Facilities Countermeasures*. *Technical Report NCEER-91-0001*, NCEER, Buffalo, NY,
39 489-496.

40 Mitsuya, M., Sakanoue, T., Motohashi, H., 2013. Beam-mode buckling of buried pipeline subjected to
41 seismic ground motion. *Journal of Pressure Vessels Technology*. 135, 1-10.

42 Mohareb, M.E., 1995. Deformational behaviour of line pipe, PhD Dissertation, University of Alberta,
43 USA.

44 National Institute of Building Science (NIBS), 2004. Earthquake loss estimation methodology. HAZUS
45 technical manual. Federal Emergency Management Agency (FEMA), Washington, USA.

1 Nazemi, N., Das, S., 2010. Behavior of X60 line pipe subjected to axial and lateral deformations.
2 Journal of Pressure Vessel Technology. 132, 031701.

3 Nigam, N. C., and Jennings, P. C., 1969. Calculation of response spectra from strong-motion
4 earthquake records. *Bulletin of the Seismological Society of America*. 592, 909-922.

5 Nuttli, O.W., 1979. Seismicity of the Central United States. Geology in the siting of nuclear power
6 plants. Geological Society of America. Reviews in Engineering Geology. 4, 67-107.

7 O'Rourke M.J., 2009. Wave propagation damage to continuous pipe. Technical Council Lifeline
8 Earthquake Engineering Conference (TCLEE), Oakland, CA, June 28-July 1, Reston, VA,
9 American Society of Civil Engineers, USA.

10 O'Rourke, M.J., Castro, G., Centola, N., 1980. Effects of seismic wave propagation upon buried
11 pipelines. *Earthquake Engineering and Structural Dynamics*. 8, 455-467.

12 O'Rourke, M.J., Castro, G., Hossain, I., 1984. Horizontal soil strain due to seismic waves. *Journal of*
13 *Geotechnical Engineering, ASCE*, 110(9), 1173-1187.

14 O'Rourke, M.J., Hmadi, K., 1988. Analysis of continuous buried pipelines for seismic wave effects.
15 *Earthquake Engineering and Structural Dynamics*. 16, 917-929.

16 O'Rourke, M.J., Ayala, G., 1993. Pipeline damage due to wave propagation. *Journal of Geotechnical*
17 *Engineering*. 119(9), 1490-1498.

18 O'Rourke M.J. and Liu X., 1999. Response of buried pipelines subjected to earthquake effects.
19 University of Buffalo, USA.

20 O'Rourke, M.J., Deyoe, E., 2004. Seismic damage to segment buried pipe. *Earthquake Spectra*. 20(4),
21 1167-1183.

22 O'Rourke, M.J., Filipov, E., Uçkan, E., 2015. Towards robust fragility relations for buried segmented
23 pipe in ground strain areas. *Earthquake Spectra*. 31(3), 1839-1858.

24 O'Rourke, T.D., Steward, H.E., Gowdy, T.E., Pease, J.W., 1991. Lifeline and geotechnical aspects of
25 the 1989 Loma Prieta earthquake. *Proceedings of the Second International Conference on Recent*
26 *Advances in Geotechnical Earthquake Engineering and Soil Dynamics*, St. Louis, MO, 1601-1612.

27 O'Rourke, T.D., Palmer, M.C., 1994. The Northridge, California Earthquake of January 17, 1994:
28 Performance of gas transmission pipelines. Technical Report NCEER-94-0011. National Center for
29 Earthquake Engineering Research. State University of New York at Buffalo, USA.

30 O'Rourke, T.D., O'Rourke, M.J., 1995. Pipeline response to permanent ground deformation: A
31 benchmark case. In: Technical Council on Lifeline Earthquake Engineering, editor. *Proceeding of*
32 *the 4th U.S. Conference on Lifeline Earthquake Engineering*, Monograph No. 6, ASCE, 288-295.

33 O'Rourke, T.D., Toprak, S., Sano, Y., 1998. Factors affecting water supply damage caused by the
34 Northridge earthquake. *Proceedings of the Sixth US National Conference on Earthquake*
35 *Engineering*. EERI.

36 O'Rourke, T.D., Jeon, S.-S., 1999. Factors affecting the earthquake damage of water distribution
37 systems. *Proceedings of the Fifth US Conference on Lifeline Earthquake Engineering*, Seattle, WA,
38 ASCE, Reston, VA, 379-388.

39 O'Rourke, T.D., Jeon, S.S., Toprak, S., Cubrinovski, M., Hughes, M., Van Ballegooy, S., et al., 2014.
40 Earthquake response of underground pipeline networks in Christchurch, NZ. *Earthquake Spectra*.
41 30, 183-204.

42 Omidvar, B., Eskandari, M., Peyghaleh, E., 2013. Seismic damage to urban areas due to failed buried
43 fuel pipelines case study: fire following earthquake in the city of Kermanshah, Iran, *Natural*
44 *Hazards*. 67(2), 169-192.

45 Padgett, J.E., DesRoches, R., 2008. Methodology for the development of analytical fragility curves for
46 retrofitted bridges. *Earthquake Engineering and Structural Dynamics*. 37, 1157-1174.

- 1 Paolucci, R., Pitilakis, K., 2007. Seismic risk assessment of underground structures under transient
2 ground deformations. Pitilakis K. (ed.) *Earthquake Geotechnical Engineering*. Geotechnical,
3 Geological and Earthquake Engineering, Springer, 433-459.
- 4 Paolucci, R. and Smerzini, C., 2008. Earthquake induced transient ground strains from dense seismic
5 networks, *Earthquake Spectra*. 24(2), 453-470.
- 6 Piccinelli, R., Krausmann, E., 2013. Analysis of natech risk for pipelines: A review. JRC86630, EUR
7 26371 EN. Institute for the Protection and Security of the Citizen, Joint Research Centre, European
8 Commission, Ispra, Italy.
- 9 Pineda-Porras, O., Ordaz, M., 2003. Seismic vulnerability function for high diameter buried pipelines:
10 Mexico City's primary water system case. *Proceedings of the International Conference on Pipeline
11 Engineering Constructions*, 2:1145–1154.
- 12 Pineda-Porras, O., Ordaz, M., 2007. A new seismic intensity parameter to estimate damage in buried
13 pipelines due to seismic wave propagation. *Journal of Earthquake Engineering*. 11(5), 773-786.
- 14 Pineda-Porras, O., Najafi, M., 2010. Seismic damage estimation for buried pipelines: Challenges after
15 three decades of progress. *Journal of Pipeline Systems Engineering and Practice*. 1, 19-24.
- 16 Pitilakis, K., Alexoudi, M., Kakderi, K., Manou, D., Batum, E., Raptakis, D., 2005. Vulnerability
17 analysis of water supply systems in strong earthquakes. The case of Lefkas (Greece) and Duzce
18 (Turkey). *International Symposium on the Geodynamics of Eastern Mediterranean Active
19 Tectonics of the Aegean Region*. Istanbul, Turkey.
- 20 Pitilakis, K., Alexoudi, M., Argyroudis, S., Monge, O., Martin, C., 2006. Earthquake risk assessment of
21 lifelines. *Bulletin of Earthquake Engineering*. 4, 365-390.
- 22 Psyrras, N., Sextos, A., 2018. Safety of buried steel natural gas pipelines under earthquake-induced
23 ground shaking. A review. *Soil Dynamics and Earthquake Engineering*. 106, 254-277.
- 24 Psyrras, N., Kwon, O., Gerasimidis, S., Sextos, A., 2019. Can a buried gas pipeline experience local
25 buckling during earthquake ground shaking? *Soil Dynamics and Earthquake Engineering*. 116, 511-
26 529.
- 27 Rossetto, T., Elnashi, A., 2003. Derivation of vulnerability functions for European-type RC structures
28 based on observational data, *Engineering Structures*. 25(10), 1241-1263.
- 29 Sarvanis, G., Karamanos, S., Vazouras, P., Mecozzi, E., Lucci, A., Dakoulas, P., 2018. Permanent
30 earthquake-induced actions in buried pipelines: Numerical modeling and experimental verification.
31 *Earthquake Engineering & Structural Dynamics*. 47(4), 966-987.
- 32 Scandella L., 2007. Numerical evaluation of transient ground strains for the seismic response analysis
33 of underground structures, PhD thesis, Politecnico di Milano, Milan, Italy.
- 34 Scandella, L., Paolucci, R., 2006. Earthquake induced peak ground strains in the presence of strong
35 lateral soil heterogeneities. *Proceedings of the 1st European Conference of Earthquake Engineering
36 and Seismology*, Geneva, Switzerland, Paper No. 550.
- 37 Shakid, H., Jahangiri, V., 2016. Intensity measures for the assessment of the seismic response of buried
38 steel pipelines. *Bulletin of Earthquake Engineering*. 14(4), 1265-1284.2016
- 39 Shinozuka, M., Takada, S., and Ishikawa, H., 1979. Some aspects of seismic risk analysis of
40 underground lifeline systems. *Journal of Pressure Vessel Technology*, Transactions of the ASME,
41 101, 31-43.
- 42 Shome, N., Cornell, C.A., Bazzurro, P., Carballo, J.E., 1998. Earthquakes, records, and nonlinear
43 responses. *Earthquake Spectra*. 14, 469-500.
- 44 Takada, S., Hassani, L., Fukuda, K., 2002. Damage directivity in buried pipelines of Kobe city during
45 the 1995 earthquake. *Journal of Earthquake Engineering*. 6:1-15

1 Toprak, S., 1998. Earthquake effects on buried lifeline systems. Ph.D. thesis, Cornell University,
2 Ithaca, NY.

3 Trifunac, M.D., Tidorovska, M.I., 1997. Northridge, California, earthquake of 1994: Density of pipe
4 breaks and surface strains. *Soil Dynamics and Earthquake Engineering*, 16, 193-207.

5 Tromans, I., 2004. Behaviour of buried water supply pipelines in earthquake zones. PhD Thesis.
6 Imperial College, London.

7 Tsatsis, A., Gelagoti, F., Gazetas, G., 2018. Performance of a buried pipeline along the dip of a slope
8 experiencing accidental sliding. *Géotechnique*. 68:11, 968-988

9 Vamvatsikos, D., and Cornell, C.A., 2002. Applied incremental dynamic analysis. *Earthquake Spectra*.
10 202, 523-553.

11 Vamvatsikos, D., Cornell, C.A., 2005. Developing efficient scalar and vector intensity measures for
12 IDA capacity estimation by incorporating elastic spectral shape information. *Earthquake*
13 *Engineering and Structural Dynamics*. 34, 1573-1600.

14 Vazouras, P., Karamanos, S.A., Dakoulas, P., 2010. Finite element analysis of buried steel pipelines
15 under strike-slip fault displacements. *Soil Dynamics and Earthquake Engineering*. 30: 1361-1376.

16 Vazouras, P., Karamanos, S.A., Dakoulas, P., 2012. Mechanical behavior of buried steel pipes crossing
17 active strike-slip faults. *Soil Dynamics and Earthquake Engineering*. 41, 164-180.

18 Vazouras, P., Dakoulas, P., Karamanos, S.A., 2015. Pipe-soil interaction and pipeline performance
19 under strike-slip fault movements. *Soil Dynamics and Earthquake Engineering*. 72: 48-65.

20 Vazouras, P., Karamanos, S.A., 2017. Structural behavior of buried pipe bends and their effect on
21 pipeline response in fault crossing areas. *Bulletin of Earthquake Engineering*. 15(11), 4999-5024.

22 Wang, J., Haigh, S.K., Forrest, G., Thusyanthan, N.I., 2011. Mobilization distance for upheaval
23 buckling of shallowly buried pipelines. *Journal of Pipeline Systems Engineering and Practice*. 3(4),
24 106-114.

25 Yang, D., Pan, J., Li, G., 2009. Non-structure-specific intensity measure parameters and characteristic
26 period of near-fault ground motions. *Earthquake Engineering and Structural Dynamics*. 38, 1257-
27 1280.

28 Yun, H., Kyriakides, S., 1990. On the beam and shell modes of buckling of buried pipelines. *Soil*
29 *Dynamics and Earthquake Engineering*. 9, 179-193.

30 Zerva, A., 1993. Pipeline response to directionally and spatially correlated seismic ground motions.
31 *Journal of Pressure Vessels Technology*. 115, 53-58.

32 Zhang, Y., 2008. Failure of X52 wrinkled pipeline subjected to monotonic bending deformation and
33 internal pressure. *International Journal of Offshore Polar Engineering*. 18, 50-55.

34